Effects of partially saturated conditions on the metabolically active microbiome and on nitrogen removal in vertical subsurface flow constructed wetlands

Catiane Pelissari[a1], Miriam Guivernau[b1], Marc Viñas[b], Joan García[c], María Velasco[d], Samara Silva Souza[e], Pablo Heleno Sezerino[a], Cristina Ávila[f,g]

[a]GESAD - Decentralized Sanitation Research Group, Department of Sanitary and Environmental Engineering, Federal University of Santa Catarina, Trindade, Florianópolis, Santa Catarina, 88040-900, Brazil.

[b]GIRO - Program of Integrated Management of Organic Waste, Institute of Agrifood Research and Technology (IRTA), Torre Marimon, E-08140, Caldes de Montbui, Barcelona, Spain.

[c]GEMMA - Environmental Engineering and Microbiology Research Group, Department of Civil and Environmental Engineering, Universitat Politècnica de Catalunya-BarcelonaTech, c/ Jordi Girona, 1-3, Building D1, E-08034, Barcelona, Spain.

[d]GMA - Program of Genetics and Animal Breeding, Institute of Agrifood Research and Technology (IRTA), Torre Marimon, E-08140, Caldes de Montbui, Barcelona, Spain.

[e]INTELAB - Integrated Technologies Laboratory, Chemical and Food Engineering Department, Federal University of Santa Catarina, Trindade, Florianópolis, Santa Catarina 88040-900, Brazil.

[f]ICRA - Catalan Institute for Water Research, Scientific and Technological Park of the University of Girona, Emili Grahit, 101, E-17003 Girona, Spain.

[g]AIMEN Technology Center, c/ Relva, 27 A – Torneiros, 36410 Porriño, Pontevedra, Spain.

*Corresponding author: Catiane Pelissari

[1]Both authors contributed equally to this manuscript.

Tel: +55 4837217696

Fax: +55 4837217696

Email: catianebti@gmail.com

ABSTRACT

Nitrogen dynamics and its association to metabolically active microbial populations were assessed in two vertical subsurface vertical flow (VF) wetlands treating urban wastewater. These VF wetlands were operated in parallel with unsaturated (UVF) and partially saturated (SVF) configurations. The SVF wetland exhibited almost 2-fold higher total nitrogen removal rate (5 g TN m^{-2} d^{-1}) in relation to the UVF wetland (3 g TN m^{-2} d^{-1}), as well as a low NO_x-N accumulation (1 mg L^{-1} vs. 26 mg L^{-1} in SVF and UVF wetland effluents, respectively). After 6 months of operation, ammonia oxidizing prokaryotes (AOP) and nitrite oxidizing bacteria (NOB) displayed an important role in both wetlands. Oxygen availability and ammonia limiting conditions promoted shifts on the metabolically active nitrifying community within 'nitrification aggregates' of wetland biofilms. Ammonia oxidizing archaea (AOA) and *Nitrospira* spp overcame ammonia oxidizing bacteria (AOB) in the oxic layers of both wetlands. Microbial quantitative and diversity assessments revealed a positive correlation between *Nitrobacter* and AOA, whereas *Nitrospira* resulted negatively correlated with *Nitrobacter* and AOB populations. The denitrifying gene expression was enhanced mainly in the bottom layer of the SVF wetland, in concomitance with the depletion of NO_x-N from wastewater. Functional gene expression of nitrifying and denitrifying populations combined with the active microbiome diversity brought new insights on the microbial nitrogen-cycling occurring within VF wetland biofilms under different operational conditions.

Keywords: partially saturated layer, nitrifying-denitrifying prokaryotes, nitrification-aggregates, metabolically active microbiome, nitrogen metabolism.

1. INTRODUCTION

Constructed wetlands (CW) are consolidated systems, which have gained popularity in decentralized wastewater treatment of small communities and rural areas from industrialized and developing countries (Álvarez et al., 2017; Guittonny-Philippe et al., 2014). In the recent decades, strategies for this technology have rapidly evolved for improving the removal of various contaminants, including organic matter, nutrients, heavy metals, emerging contaminants and pathogenic organisms, by implementing a diverse range of wetland configurations (Ávila and García, 2015; Nivala et al., 2013).

Nitrogen is a nutrient that plays a crucial role in the biology of living organisms, but it becomes a serious problem when an excess of reactive nitrogen is released to the environment, due to associated environmental and public health concerns (WEF, 2010). In urban wastewater treatment plants (WWTP), complete nitrogen removal is commonly achieved via autotrophic nitrification and heterotrophic denitrification: the so-called nitrification-denitrification (NDN) process that is mainly conducted by nitrifying and denitrifying populations. In the presence of oxygen, nitrification is a two-step process where ammonia-oxidizing prokaryotes (AOP) oxidize NH_4^+ to NO_2^- by the ammonia monooxygenase (AMO) enzyme, and nitrite-oxidizing bacteria (NOB) oxidize NO_2^- to NO_3^- by the nitrite oxidoreductase (NXR) enzyme. Despite the fact that N_2O is formed as an intermediate by heterotrophic denitrifying bacteria, it is noteworthy to mention that N_2O is also produced as by-product of ammonia oxidation, so that AOP represent a primary source of this potent greenhouse gas (Yoon et al., 2016).

A frequent limitation in single-stage CW systems is the elimination of total nitrogen (TN), since neither the vertical (VF) nor the horizontal (HF) subsurface

flow CW provide the appropriate conditions to enable the combined process in a single treatment step (Saeed and Sun, 2012; Vymazal, 2013). In order to solve this drawback different strategies and intensifications have been established, such as the combination of different CW types, known as hybrid systems, the recirculation of the final effluent, the use of intermittent aeration or the implementation of fill-and-drain cycles (Ávila et al., 2017; Foladori et al., 2013; Hu et al., 2014; Vymazal, 2013; Wu et al., 2014). However, such improvements need additional energy inputs or further land requirements, thus increasing the cost and carbon footprint of the technology.

The partial saturation of the bottom part of the typically unsaturated vertical subsurface flow (UVF) wetland has recently emerged as a promising alternative for the improvement of TN removal, without the need of additional energy nor land area. The promotion of the co-occurrence of aerobic and anoxic/anaerobic conditions within a single CW unit could enhance the NDN activity (Pelissari et al., 2017a). A few examples of partially saturated vertical flow wetlands (SVF) have shown satisfactory results, with TN removal efficiencies ranging from 40 - 70% (Dong and Sun, 2007; Huang et al., 2017; Pelissari et al., 2017a; Saeed and Sun, 2017).

Despite the fact that microbial transformations play a major role in contaminant removal in the CW systems, the biodiversity and functional aspects of the CW microbiome are scarcely known (Button et al., 2016). Recent studies evaluating TN removal in CW, have concluded that the knowledge of biofilm dynamics and structure is essential to set operational conditions, which are also linked with seasonal variations (Faulwetter et al., 2009; Pelissari et al., 2017a, b).

AOP are phylogenetically restricted to the three bacterial genera: *Nitrosococcus*

(*Gammaproteobacteria*), *Nitrosomonas* (including *Nitrosococcus mobilis*, which phylogenetically belongs to *Nitrosomonas*) and *Nitrosospira* (both *Betaproteobacteria*) and members of the archaeal phylum *Thaumarchaeota*. Oppositely, NOB are more diverse, including the genera *Nitrobacter, Nitrotoga* and *Nitrococcus* belonging to *Alpha*-, *Beta*- and *Gammaproteobacteria*, respectively, and four additional genera assigned to *Nitrospira* (*Nitrospirae* phylum), the marine NOB *Nitrospina* and *Candidatus Nitromaritima* (*Nitrospinae* phylum), and *Nitrolancea* (*Chloroflexi* phylum) (Palomo et al., 2017).

Considering the possible interaction among microbial communities in nitrifying biofilms, the so-called 'nitrification aggregate' was recently postulated (Daims et al., 2016). This is a complex network composed by AOP and NOB populations that have a tight interaction owing to the close spatial co-aggregation. Metabolites are exchanged using short diffusion pathways, thus minimizing the loss and maximizing the effectiveness of substrate use (Flemming et al., 2016). Nevertheless, the capacity of complete ammonia oxidation (COMAMMOX) by a single *Nitrospira* in the presence of a specific AMO (ammonium monooxygenase) enzyme has been recently reported (Daims et al., 2015).

On the other hand, heterotrophic denitrifiers use NO_3^-, NO_2^-, NO and N_2O catalyzed by enzymes encoded by *nar*, *nir*, *nor*, and *nosZ* genes (Brenzinger et al., 2015). According to the nitrous oxide reductase encoding gene (*nosZ*), bacteria capable of N_2O reduction to N_2 are grouped in two clades on the basis of *nos* operon structures and *nosZ* sequences. These two phylogenetically distinct *nosZ* clades, clade I and II, are classified as typical and atypical denitrifiers, respectively. Both clades exhibit distinct features by differing in kinetic properties (Yoon et al., 2016). The typical denitrifiers mainly belong to *Alpha*-,

Beta-, and *Gammaproteobacteria*, and the atypical denitrifiers encompass different phyla, including *Bacteroidetes*, *Firmicutes* or *Epsilonproteobacteria* (Jones et al., 2013). Moreover, genome analysis revealed that most of the typical denitrifiers are capable of complete denitrification, whereas atypical denitrifiers, that are suggested as N_2O sinks, possess a more-diverse nitrogen metabolism, including dissimilatory nitrate reduction to ammonium (DNRA) and missing the NO-generating nitrite reductase genes *nirK* and *nirS* (Orellana et al., 2014). In any case, *nosZ* genes are pH-dependent, with high values promoting N_2O consumption and low values its accumulation (Brenzinger et al., 2015).

DNA/RNA-based assessments by Reverse Transcription and Quantitative Polymerase Chain Reaction ((RT)-qPCR) and Next Generation Sequencing (NGS) could elucidate the total and metabolically active microbial populations attached to the granular material of CW. Several studies have focused their research on the nitrifying population dynamics taking place within the filter bed of UVF and SVF wetlands (Pelissari et al., 2016; 2017a,b; Tietz et al., 2007). Besides the above-mentioned nitrification-denitrification processes, other nitrogen transformation pathways have been established in different UVF and SVF wetlands, such as the anaerobic ammonium oxidation (ANAMMOX), partial NDN process, complete autotrophic nitrogen-removal over nitrite (CANON), and heterotrophic nitrification-aerobic denitrification (Austin et al., 2006; Dong and Sun, 2007; Fan et al., 2016; Hu et al., 2016; Huang et al., 2017).

A recent assessment of microbial community dynamics in a nitrifying UVF wetland (typically unsaturated) was conducted at DNA/RNA level (Pelissari et al., 2017b). The results of that study showed that AOA were more active than AOB and denitrifying bacteria at expression level (RNA counts), whereas AOB were

more abundant than AOA (DNA counts). However, further research is needed to elucidate the distribution of metabolically active nitrifying and denitrifying microbial populations occurring within the biofilms of VF wetlands.

This study aims at assessing the AOB/AOA/NOB and denitrifying bacteria interactions within the biofilms of two VF wetlands (conventional unsaturated and partially saturated bed) treating urban wastewater. For this purpose, the treatment performance was monitored during six months in terms of physicochemical and microbiological analyses (at DNA and RNA levels). Correlation analyses between environmental gradients and nitrifying population dynamics will provide a deeper insight into the interrelationships between nitrogen cycle and microbial ecology in CW.

2. MATERIALS AND METHODS

2.1. Description of the treatment system

The experimental treatment plant was set outdoors at the experimental facility of the GEMMA group (Department of Civil and Environmental Engineering of the Universitat Politècnica de Catalunya BarcelonaTech, Spain) in a Mediterranean climate. The treatment system was comprised by an Imhoff tank (0.2 m^3, hydraulic retention time = 12h), followed by an UVF and a SVF wetland operated in parallel (Fig. 1). Each wetland had a surface area of 1.5 m^2 (1.0 m × 1.5 m), and a bed media depth of 0.8 m. This consisted of a 0.1 m sand layer (Ø= 1-2 mm) in the top and 0.7 m of fine gravel (Ø= 3-8 mm) underneath. Both wetlands were constructed in polyethylene tanks, and a polyethylene pipe distributed the pumped wastewater evenly 0.1 m above the top of the bed. Feeding was performed every day by means of intermittent pumping, totaling eight pulses

along the day (25 L $pulse^{-1}$), with an approximate duration of two min per pulse. In this study, UVF and SVF wetlands did not operate with rest periods, as the study conducted by Sezerino et al. (2012).The macrophyte employed in both wetlands was *Phragmites australis*, which was very well developed at the time of the study.

At the beginning of the implementation of the partial saturation in the SVF wetland (Jan 2016), both wetlands had been continuously working unsaturated (under higher organic loads) and alternating feed-rest cycles since the system's commissioning in 2010 (Ávila et al., 2017, 2016; Pelissari et al., 2017b). In the current study, whereas the UVF wetland was operated typically unsaturated (i.e. 0.8 m free drainage), the SVF wetland had the bottom part (0.35 m) saturated (43% of total depth) by setting the outlet pipe at that height. Adjustment of the saturation height was carried out beforehand, where 0.45 m of saturation originated insufficient nitrification of ammonia. Each wetland received a flow of 200 L d^{-1}, resulting in average organic (OLR) and hydraulic loading rates (HLR) of 40 g COD m^{-2} d^{-1} and 133 mm d^{-1}, following recommendations by Sezerino et al. (2012).

An electromagnetic flow meter (Sitrans F M Magflo) was installed at the inlet and outlet of the wetland units to monitor flow values in the treatment system, and accordingly water quality parameters were expressed on a mass balance basis. Evapotranspiration was estimated based on influent and effluent volumes of each wetland, measured by electromagnetic flow meters.

2.2. Sampling and analysis of conventional water quality parameters

Physicochemical data from influent and effluent water samples were determined twice a week for 6 months (Jan-Jul 2016) by taking grab samples at 10 am, after a feeding pulse in both wetlands. Onsite measurements of water temperature, dissolved oxygen (DO), pH and electrical conductivity (EC) were taken by using a Digital Termometer (Hanna Checktemp-1), a DO6 Oxymeter (Eutech EcoScan), a pH-Meter (Crison Instruments) and a conductivity meter (Endress+Hauser CLM 381), respectively. Redox potential (E_H) was also analyzed onsite by using a Redox Meter (Thermo Scientific Orion 3-Star) and values obtained were corrected for the potential of the hydrogen electrode. The determination of conventional wastewater quality parameters, including chemical oxygen demand (COD), total suspended solids (TSS) and ammonia nitrogen (NH_4-N) was done following the Standard Methods (APHA, 2012). Total nitrogen (TN) and total organic carbon (TOC) were analyzed using a Multi N/C analyzer (Analytik Jena 2100 S). Oxidized nitrogen species (NO_x-N) and sulfate (SO_4^{2-}) were determined using a chromatography system (Dionex ICS-1000).

2.3. Microbial community assessment and samples campaigns

For the microbiological assessment, samples were taken in triplicate from influent wastewater, as well as from the biofilm of top (0-15 cm depth) and bottom (70-80 cm depth) layers of the bed media from both wetlands. In order to evaluate the changes caused by the saturation of the bed within the SVF wetland, sampling was performed in two campaigns, at the start (T0 - a day before the bottom saturation) and at the end (TF - after 6 months of operation) of the study (Jan and Jul 2016). For the UVF wetland, samples were collected at the end of the study (TF - Jul 2016). The data from biofilm sampling for the initial period of UVF

wetlands (Table S1) refers to the previous studies conducted by Pelissari et al. (2017b).

In order to elucidate the nitrogen transforming microbial communities occurring in both wetlands, a DNA/RNA-based assessment was carried out by quantifying functional genes, and the microbial community structures of influent wastewater and wetland biofilms were determined by Next Generation Sequencing (NGS). Reverse transcription and quantitative polymerase chain reaction ((RT)-qPCR) of AOP (*amoA* of AOB and AOA) and typical denitrifiers (*nosZ* – clade I) were performed in the biofilm from both wetlands. Moreover, active bacterial and archaeal microbial communities were deeply assessed by means of 16S rRNA-based high throughput sequencing in MiSeq Illumina Platform. This analysis allowed the identification of the metabolically active microbial diversity enriched in the biofilm of UVF and SVF wetlands' filter media throughout the bioprocess.

Simultaneous RNA/DNA extractions, qPCR analysis and NGS performance are detailed in the supplemental material (SM) (Text S1, S2, and S3). Data from MiSeq NGS assessment were submitted to the Sequence Read Archive (SRA) of the National Center for Biotechnology Information (NCBI) with the accession number SRP095451, for active bacterial and archaeal populations.

2.4 Statistical data analyses

The Shapiro-Wilk test was performed on conventional wastewater quality parameters to determine whether data were normally distributed. Given that data did not follow a normal distribution and considering their paired structure, Friedman tests were performed to compare DO, EC, E_H, pH and concentrations of TSS, COD, TOC, TN, NH_4-N, NO_x-N and SO_4^{2-} between influent and effluents

of SVF and UVF wetlands. Moreover, evapotranspiration (mm d^{-1} and %), load removal rate (LRR) and load removal efficiency (LRE) of TSS, COD, TN, NH_4-N and SO_4^{2-} were compared between SVF and UVF effluents with a Wilcoxon signed rank test which also took into account the paired structure of the measures. The significance threshold was established at 0.05 type I error.

The Shapiro-Wilk test was also performed on the normalization of transcripts to 16S rRNA gene copies (*nosZ* transcripts/16S rRNA genes, *amoA*_AOA transcripts/16S rRNA genes and *amoA*_AOB transcripts/16S rRNA genes), and on the specific activity ratios (*nosZ* transcripts/ *nosZ* genes, *amoA*_AOA transcripts/ *amoA*_AOA genes and *amoA*_AOB transcripts/*amoA*_AOB genes), to determine whether they were normally distributed. According to normal distribution, an analysis of variance (ANOVA) including the combination of the following factors: wetland (UVF and SVF), layer (bottom and top) and time of the operation in the case of SVF wetland (T0 and TF), was performed for each normalization and activity ratio. Subsequently, pairwise comparisons (Fisher's least significant difference (LSD)) were applied to test differences between (i) top and bottom layers at the start (T0) of the operation in SVF wetland and at the end (TF) of the operation in both wetlands; (ii) the start and the end of the operation of both layers in the SVF wetland; (iii) UVF and SVF wetlands in both layers at the end of operation. The significance threshold was established at 0.05 type I error.

Spearman's ranked correlation test was performed in order to study the monotonicity and the strength of the correlations between i) the relative abundances (RA) of the operational taxonomic units (OTUs) taxonomically assigned to well-known NOB, *Nitrobacter* spp. and *Nitrospira* spp (>80%

bootstrap RDP) identified by cDNA-based NSG assay (Table S2), as well as, ii) the logarithm of the number of transcripts of *amoA* of AOB and AOA obtained from (RT)-qPCR and the RA of NOB identified by NGS data. For these tests, data from a previous study conducted in the same UVF wetland from Pelissari et al. (2017b), were also included (Table S1).

To evaluate the population diversity of active bacterial and archaeal populations, the number of OTUs, the inverted Simpson index, Shannon index (H), Goods coverage and Chao1 richness estimator were calculated by using the Mothur software v.1.34.4 (http://www.mothur.org). All the estimators were normalized to 50,000 reads within the range of the lowest number of reads among the different samples. Moreover, multiple correspondence analysis (MCA) of MiSeq data (relative OTU distribution matrix) was performed in order to know which were the OTUs that contributed the most to clusterization of samples.

All statistical analysis were performed by means of XLSTAT 2018 software (Addinsoft, Paris, France) and SigmaPlot 11.0 software.

3. RESULTS AND DISCUSSION

3.1 Treatment performance of the unsaturated and partially saturated vertical flow constructed wetlands

Physicochemical parameters of influent wastewater and the effluents of two wetlands operated in parallel for six months (Jan-Jul 2016) are presented in Table 1. Differences in E_H, pH and DO between wetlands' effluent resulted statistically significant ($P < 0.05$), showing the SVF wetland lower values in all cases and displaying a greater variation throughout the study. Moreover, the temperature of SVF effluent was slightly increased compared to the influent wastewater (Table

1) but differences were not significant (P_{T^a}= 0.068). Nonetheless, this effect could be explained by the higher retention time of the wastewater in this unit, considering that both wetlands were constructed above the ground and were exposed directly to the sun. Furthermore, the saturated layer in the SVF wetland promoted a significant (P < 0.05) lower effluent volume than the UVF unit due to higher evapotranspiration rates. These results are associated with a better adaptation of the vegetation in the SVF unit, which showed greater plant height and growth.

TSS removal was moderate in the two wetlands (about 70% of LRE), and both units exhibited similar LRR (about 10 g TSS m^{-2} d^{-1}). COD LRE was similar for both units (about 65%). Moreover, the difference between both CW in the COD removal was not statistically significant (P < 0.05), showing that the decrease of the aerobic filter volume in the SVF wetland compared to the UVF wetland did not hamper the elimination of organic matter. A similar behavior was reported in a previous study, where two CW were operated in parallel with a similar mean COD removal efficiency of 72% for UVF and SVF wetlands (Dong and Sun, 2007).

Different nitrogen transformations occurred in the UVF and SVF wetlands owing to the specific conditions of each configuration (Saeed and Sun, 2012). On the one hand, no statistical differences were observed for NH_4-N LRE (about 69% in both wetlands; P = 0.928), indicating that the nitrification process was not affected by the partial saturation of the filter bed in the SVF wetland (Table 1). Although the effluents of both CW had similar NH_4-N concentrations (6 mg L^{-1}), the lower oxygenated conditions of the SVF wetland would result in a lower mineralization of the organic nitrogen (Kadlec and Wallace, 2009).

On the other hand, the concentration of oxidized nitrogen species was significantly greater ($P < 0.05$) in the effluent of the UVF wetland (26.24 ± 7.85 mg NO_x-N L^{-1}) than in the SVF wetland (0.89 ± 0.94 mg NO_x-N L^{-1}), indicating a higher denitrification process in the SVF wetland (Table 1). This finding is in agreement with a study performed in a full scale SVF wetland (Pelissari et al., 2017a). As a result, the SVF unit achieved a significantly higher TN LRE (56%) than the UVF wetland (34 %) ($P < 0.05$). The TN LRR of the SVF wetland (4.9 ± 1.6 g TN m^{-2} d^{-1}) are in agreement with average values reported for hybrid systems containing subsurface (VF + HF) flow CW in series (4.2 ± 5.1 g TN m^{-2} d^{-1}) (Vymazal, 2013). According to the results obtained, the bottom layer saturation effectively promotes the occurrence of an optimized NDN process within a single wetland unit, thus enhancing TN removal without further land or energy requirements.

Finally, sulfate removal was also significantly higher ($P < 0.05$) in the SVF wetland (Table 1) both in concentration and LRE. The saturated conditions of this unit promoted appropriate redox potentials, which linked with carbon availability (Fig. S1), enriched sulfate-reducing bacteria (SRB) such as *Desulfobacterales* and *Desulforomonadales* (see Fig 2a), subsequently enabling sulfate removal. In contrast, the oxidative character of the UVF wetland presumably promoted the oxidation of hydrogen sulfite of the wastewater (Faulwetter et al., 2009; Chen et al., 2016), which resulted in a higher sulfate concentration in the UVF effluent compared to the influent. This has also been observed in previous studies within this treatment plant (Ávila et al., 2016).

3.2 Active microbial community structure in the unsaturated and partially

saturated vertical flow constructed wetlands

3.2.1 Global diversity of active microbial communities

The alpha diversity of the active bacterial populations in biofilms of filter media was clearly higher than that observed in the influent wastewater, with a Shannon index of 6.45 - 6.77 (4.25 in the influent wastewater) and inverted Simpson index of 138.43 – 210.74 (14.92 in the influent wastewater). All biofilms maintained high diversity values (i.e. H above 6.2 and Chao1 above 4100) even at late stages, which would confirm the presence of a mature and metabolically active bacterial community structure in both CW. Alpha diversity was also quite similar (i.e. H values of 6.45 - 6.27 and 6.77 - 6.63 for SVF and UVF units, respectively) when top and bottom layers were compared. A slight decrease of the diversity was depicted in the bottom layer of the SVF wetland with respect to initial conditions (T0), which could indicate a specialization of certain microbial communities under anoxic conditions (Fig. 2, 3 and Table 2).

Globally, the diversity of the active archaeal populations in bed biofilms was much lower than that observed for bacteria, and different in both CW. Richness values were 10-40 fold lower (OTUs: 72 - 124 per sample) than those observed in bacteria, and at the same range than that depicted in influent wastewater (i.e. Chao1 of 100 - 161 in the CW biofilms and influent wastewater). Archaeal diversity was clearly higher in the SVF (H: 1.74 - 2.02) than in the UVF wetland (H: 0.76 - 1.08). Such kind of differences could be explained by the co-occurrence of methanogens (*Methanotrichaceae* and *Methanobacteriaceae*) and AOA (*Nitrososphaeraceae*) at all depths of the SVF wetland (Fig. 2). Interestingly, metabolically active AOA populations (*Nitrososphaera* in both CW, and *Nitrosopumilus* in the UVF wetland) were enriched in both CW (15 - 99% of RA),

in comparison with influent wastewater (0.2% of RA, Fig. 2).

3.2.2 Multivariate statistical analysis and active microbiome structure

Multiple correspondence analysis (MCA) of the OTUs distribution of metabolically active bacteria and archaea populations revealed that the microbial composition was different in the CW and bed depths, being clearly affected after 6 months of implementation of the saturated layer in the SVF wetland (Fig. 2 and 3).

Concerning the bacterial population (Fig. 3a), influent wastewater (Influent_TF) samples were clustered rather distantly from CW biofilm samples due to a high predominance of OTU1 (*Pseudomonas*), OTU10 (*Dechloromonas*) and OTU3 (*Ohtaekwangia*), which could be linked to favorable anaerobic conditions for denitrification at the Imhoff tank. Moreover, UVF wetland samples (UVF_top_TF and UVF_bottom_TF) were also clustered far from the SVF wetland ones (SVF_top_T0,TF and SVF_bottom_T0,TF), mainly due to the differential activity of OTU4 (*Streptomyces*) and OTU7 (*Nitrospira*) linked to aerobic metabolism, which was in agreement with the activity of aerobic archaea in the UVF wetland. Oppositely, SVF wetland communities were differentially enriched in *Nitrobacter* activity (OTU5) and *Clostridium* XI (OTU2). Predominant OTUs (>1% RA) are summarized in Table S3 and S4 for bacterial and archaeal populations, respectively.

In relation to the archaeal population (Fig. 3b), MCA analysis revealed that the diversity structure of SVF and UVF wetlands were different mainly by a selective enrichment at TF of active methanogenic archaea in SVF unit in both layers, and the AOA enrichment in the UVF wetland. The SVF wetland promoted the enrichment of methanogenic archaea such as *Methanosaeta* (OTU1, Fig. 3b) in the bottom (80% of RA) and top layers (60% of RA) (Fig. 2), confirming the

405 presence of anaerobic conditions. On the other hand, archaeal communities in
406 the UVF wetland were dominated by AOA (99% of RA) throughout the CW depth.
407 OTU2 belonging to *Nitrososphaera* (Fig. 2 and 3) were the most different OTU in
408 the MCA analysis of the UVF wetland. The occurrence of active ribotypes
409 belonging to well-known AOA, such as *Nitrososphaera* (90-80% RA) and
410 *Nitrosopumilus* (10-20% of RA, Fig. 2) at top and bottom layers of the UVF
411 wetland would confirm the existence of oxic conditions throughout the filter depth.
412 This fact is in line with the lack of efficient denitrifying activity (NO_x-N
413 accumulation in the effluent) in this CW, with high organic nitrogen hydrolysis and
414 therefore available ammonia for nitrifiers. It is worth noting that the high RA of
415 methanogenic archaea (such as *Methanosaeta* (OTU1, Fig. 3b)) in the SVF
416 wetland could be a good indicator of anaerobic conditions in this unit.

417 Concerning the nitrifying populations, the NOB attached to the UVF wetland
418 biofilm was represented by *Nitrobacter* and *Nitrospira* OTUs. In relation to the
419 previous study from the same UVF wetland (Pelissari et al., 2017b, Table S1),
420 *Nitrobacter* suffered a prominent decrease from 3-4% down to 1% RA.
421 Meanwhile, the other well-known NOB represented by *Nitrospira* genus,
422 experimented an increase accounting from 0.1 to 0.5% at the top and from 2 to
423 2.5% RA at the bottom layer (Table S2). This NOB population shift could be
424 presumably explained either by seasonal factors or by the lower OLR, which
425 could generate a microaerophilic environment favoring the *Nitrospira* population
426 (Huang et al., 2010). *Nitrospira*-like bacteria were postulated as *K*-strategist with
427 a higher affinity than *Nitrobacter* to nitrite and oxygen, reaching high densities
428 under substrate limiting conditions (Schramm et al., 1999). Recent studies
429 showed the different behavior between *Nitrospira* lineages (Koch et al., 2015)

under varying physicochemical conditions, such as nitrite concentrations or availability of organic substrates (Maixner et al., 2006). It is also worth mentioning that AOB families of UVF wetland biofilms were found with RA below 0.1% (Table S5), which agrees with the *amoA*_AOB qPCR results described below.

3.2.3 Dynamics of nitrifying and denitrifying microbial populations

The operational characteristics of the CW clearly affected the AOP community, and more in particular the AOA population (Fig. 4, S2 and S3, Text S4 and S5). Quantitative results revealed that AOA was the main metabolically active AOP population in both CW (Fig. 4, S2 and S3, Text S4), with highest activity ratios (transcripts/gene copies) and normalized transcripts to 16S rRNA genes (transcripts/16S rRNA gene copies). However, at the ending period of SVF wetland (TF), AOA were considerably reduced, whereas metabolically active AOB experimented a significant ($P < 0.05$) enrichment (Fig. 4b), outcompeting AOA in the bottom layer. This fact could be explained by the nitrifier-denitrification capacity of AOB in oxygen limiting conditions (Stieglmeier et al., 2014).

Environmental parameters are critical for the AOP community development. AOB are described to be rather resilient to high influent ammonium concentrations, toxic compounds and pH changes (Fan et al., 2016; Webster et al., 2002). In addition, AOB are commonly found in industrial WWTP with high ammonium concentrations (36 - 422 mg L^{-1}) (Cydzik-Kwiatkowska et al., 2016; Limpiyakorn et al., 2011). Nevertheless, it is important to keep in mind that DNA/RNA-based assays are essential to reaffirm the tendency of AOB/AOA dynamics in a biofilm aggregation, and more in particular in CW biofilms. In the present study, influent

SUPPLEMENTARY MATERIAL

Effects of partially saturated conditions on the metabolically active microbiome and on nitrogen removal in vertical subsurface flow constructed wetlands

Catiane Pelissari[a1], Miriam Guivernau[b1], Marc Viñas[b], Joan García[c], María Velasco[d], Samara Silva Souza[e], Pablo Heleno Sezerino[a], Cristina Ávila[f,g]

[a]GESAD - Decentralized Sanitation Research Group, Department of Sanitary and Environmental Engineering, Federal University of Santa Catarina, Trindade, Florianópolis, Santa Catarina, 88040-900, Brazil.

[b]GIRO - Program of Integrated Management of Organic Waste, Institute of Agrifood Research and Technology (IRTA), Torre Marimon, E-08140, Caldes de Montbui, Barcelona, Spain.

[c]GEMMA - Environmental Engineering and Microbiology Research Group, Department of Civil and Environmental Engineering, Universitat Politècnica de Catalunya-BarcelonaTech, c/ Jordi Girona, 1-3, Building D1, E-08034, Barcelona, Spain.

[d]GMA - Program of Genetics and Animal Breeding, Institute of Agrifood Research and Technology (IRTA), Torre Marimon, E-08140, Caldes de Montbui, Barcelona, Spain

[e]INTELAB - Integrated Technologies Laboratory, Chemical and Food Engineering Department, Federal University of Santa Catarina, Trindade, Florianópolis, Santa Catarina 88040-900, Brazil.

[f]ICRA - Catalan Institute for Water Research, Scientific and Technological Park of the University of Girona, Emili Grahit, 101, E-17003 Girona, Spain.

[g]AIMEN Technology Center, c/ Relva, 27 A – Torneiros, 36410 Porriño, Pontevedra, Spain.

*Corresponding author: Catiane Pelissari

[1]Both authors contributed equally to this manuscript.

Tel: +55 4837217696

Fax: +55 4837217696

Email: catianebti@gmail.com

Text S1. Simultaneous RNA/DNA extraction. All samples collected were immediately mixed with 2 mL of LifeGuard Reagent (MO BIO) to prevent RNA degradation. Simultaneous DNA/RNA extraction from approximately 0.25 g of the filter bed and the pellet from 1 mL of water samples (20.000g/5' at 4ºC) were extracted in triplicate for each period by using an adapted protocol of PowerMicrobiome™ RNA Isolation kit, (MO BIO Laboratories, Inc., Carlsbad, CA). The RNA extracts were treated for 10 min at 25°C with 10 units of DNase I (a room temperature stable DNase enzyme from the same PowerMicrobiome Isolation kit) to remove any contaminating genomic DNA. All of the DNase I-treated RNAs were subjected to 16S rRNA-based PCR amplification to detect DNA impurities. Purified RNAs were transcribed to cDNA with PrimeScript™ RT reagent Kit (Perfect Real Time, Takara) following the manufacturer's instructions. cDNA and DNA extracts were kept frozen at -80ºC until further analysis.

Text S2. Quantification of the total and metabolically active nitrifying and denitrifying population by (RT)-qPCR. Quantitative analysis of total versus active bacterial population was conducted in the V3 hypervariable region of 16S rRNA as elsewhere described in Prenafeta Boldú et al. (2012). Ammonia monooxygenase α-subunit encoding genes of AOB population (a*moA*_AOB) were quantified as previously reported by Rotthauwe et al. (1997). *amoA* of AOA population was quantified by a new combination of primers in order to match all known AOA as previously described in Pelissari et al. (2017). Denitrifying populations were quantified by *nosZ* gene (clade I), the encoding gene of the catalytic subunit of nitrous oxide reductase, as previously reported in Calderer et al. (2014). All qPCR reactions were conducted in a Real Time PCR System

MX3000P (Stratagene, La Jolla, CA) and all samples were analyzed in triplicate by means of three independent cDNA/DNA extracts.

The standard curve of each target gene was designed by using FunGene data base (http://fungene.cme.msu.edu/) gBlocks® Gene Fragments (IDT, Integrated DNA Technologies). Ten-fold serial dilutions of synthetic genes were subjected to qPCR assays in duplicate showing a linear range between 10^1 and 10^8 gene copy numbers per reaction to generate standard curves. qPCR reactions fitted quality standards: efficiencies were between 90-110% and R^2 above 0.985. All results were processed by MxPro™ QPCR Software (Stratagene, La Jolla, CA) and were treated statistically.

Text S3. Microbial diversity of metabolically active bacterial and archaeal populations. High-throughput analysis was performed to find out those most prevalent active eubacterial and archaeal populations in the influent wastewater, and in bed materials at different depths in the UVF wetland (at the end of the operational period) and SVF wetland (at start and end). 16S rRNA (cDNA) massive libraries were prepared and sequenced at Molecular Research MR DNA Laboratory (Shallowater, TX, USA). High throughput sequencing analysis was carried out in a MiSEq Illumina Platform. For the eubacterial 16S rRNA libraries, the primer set was 27F (5'-AGRGTTTGATCMTGGCTCAG–3') / 519R (5'-GTNTTACNGCGGCKGCTG-3') and for the archaeal was 349F (5'-GYGCASCAGKCGMGAAW-3') / 806R (5'–GGACTACVSGGGTATCTAAT-3').

The obtained reads were compiled in FASTq files for further bioinformatic processing. Trimming of the 16S rRNA barcoded sequences into libraries was carried out using QIIME software version 1.8.0 (Caporaso et al., 2010a).

Sequences were denoised and chimeras were removed (Caporaso et al., 2010b; Haas et al., 201; Reeder and Knight, 2010). Quality filtering of the reads was performed at Q25, prior to the grouping into Operational Taxonomic Units (OTUs) at a 97% sequence homology cut-off. OTUs were then taxonomically classified using BLASTn against GreenGenes and RDP (Bayesian Classifier) database and compiled into each taxonomic level (De Santis et al., 2006).

Regarding bacteria, diversity calculations were normalized to 50,000 contigs (MiSeq 16S contigs) (from 56,415 to 72,023), with a good coverage (0.988 to 0.977). Richness values were high in the influent wastewater (Chao1: 2333) but clearly higher in biofilms (Chao1 of 4,165-4,831) at all depths and both wetlands, encompassing a total of 7,312 different OTUs in the whole study (1,587-3,913 OTUs per sample). Concerning archaeal populations, diversity and richness calculation were normalized to 25,000 contigs (MiSeq reads) because of lower number of clean 16S-archaea contigs (25,978-122,818), but still with a good coverage (0.998 to 0.999).

Text S4. Microbial community results from unsaturated vertical (UVF) subsurface flow constructed wetland. At the ending (TF) period of UVF wetland, total eubacterial population attached at biofilm from bed media were actively detected in both layers (10^{11} 16S rRNA transcripts g^{-1}). Regarding *amoA* gene expression, AOA were revealed as the main metabolically active AO population in all depths achieving 10^6 and 10^5 *amoA* transcripts g^{-1} in the top and bottom layer, respectively, whereas, only 10^2 and 10^3 *amoA* transcripts g^{-1} of AOB were detected in the top and bottom layer, respectively. Therefore, AOA were again predominantly active in the same range compared to a previous study

conducted with the same UVF wetland unit running under higher ORL and HLR (Pelissari et al., 2017).

Remarkable differences of metabolically active bacteria and archaea populations found in the influent and in biofilm grown on bed media were observed. At class level bacterial population profile of influent wastewater was dominated by *Gammaproteobacteria* (34% RA) and *Betaproteobacteria* (28% RA), while *Actinobacteria* and *Alfaproteobacteria* (20% RA) were selectively enriched on the bed biofilm, at all depths. In filter media biofilms the microbial community was actively dominated in depth (top - bottom layer), by *Actinobacteria* (22%-20% RA), *Alfaproteobacteria* (20%-19% RA), *Planctomycetia* (13%-11% RA), *Deltaproteobacteria* (7%-10% RA), *Ktedonobacteria* (1%-7% RA), Gammaproteobacteria (3%-2% RA), *Acidobacteria* Gp4 (3%-2.5% RA) and *Nitrospira* (2.5%-2% RA) classes.

Text S5. Microbial community results from partially saturated vertical (SVF) flow constructed wetland. After 6 months of operation of SVF wetland, bacteria population was more active in top than in bottom layer (10^{12} and 10^{11} 16S rDNA transcripts g^{-1}, respectively), due to greater availability of carbon and nutrients with the consequent higher stimulation of microbial growth. The saturation conditions of bottom layer giving less oxygen accessibility (0.7 mg $O_2 \cdot L^{-1}$ SVF wetland effluent versus 2.2 mg O_2 L^{-1} UVF wetland effluent) resulted in a biomass decrease respect starting period.

During the startup of SVF wetland, AOA exerted more activity than AOB, being two orders of magnitude superior in both layers (10^7 *amoA*_AOA and 10^5

*amoA*_AOB transcripts g^{-1} in both layers, respectively). In addition, different metabolically active diversity profiles were observed in biofilms through depth and time. At starting period, *Alphaproteobacteria* (27%-28% RA), *Deltaproteobacteria* (18%-5% RA) and *Planctomycetia* (11%-16% RA) were the predominant active populations in both layers respectively, whereas after 6 months, *Alphaproteobacteria* (20%-18% RA) and *Deltaproteobacteria* (7%-4% RA) were reduced.

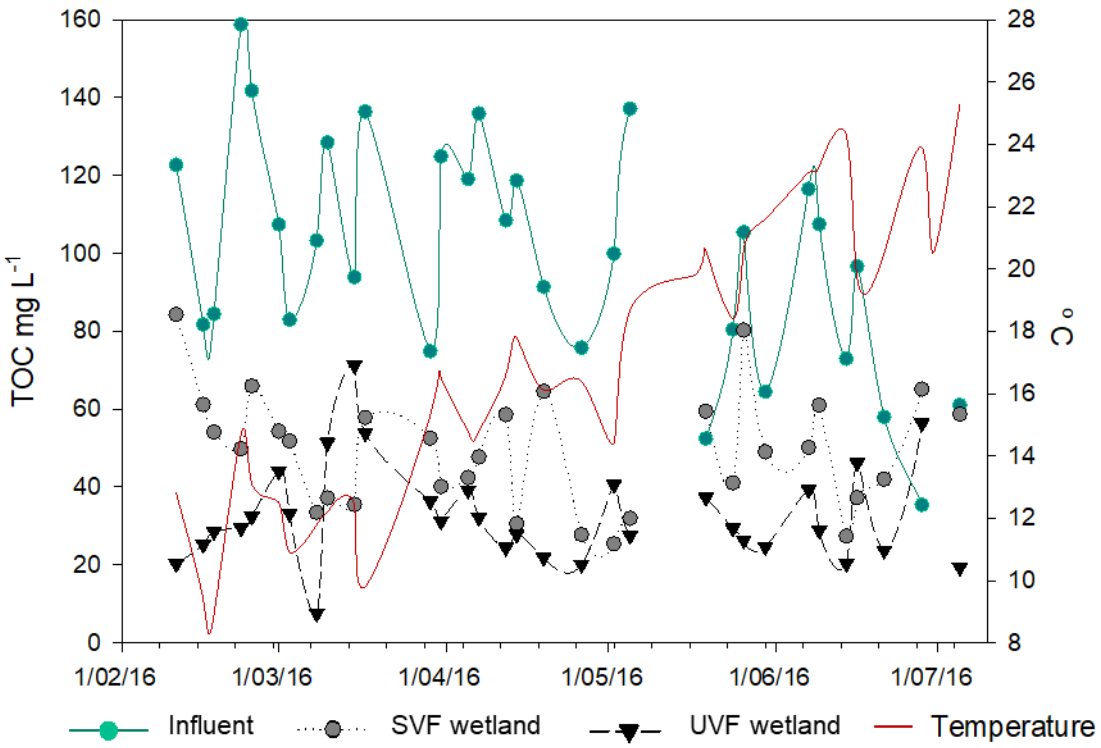

Figure S1. TOC concentrations and temperature identified in the influent and effluent from unsaturated vertical (UVF) and partially saturated (SVF) vertical flow wetlands throughout the study.

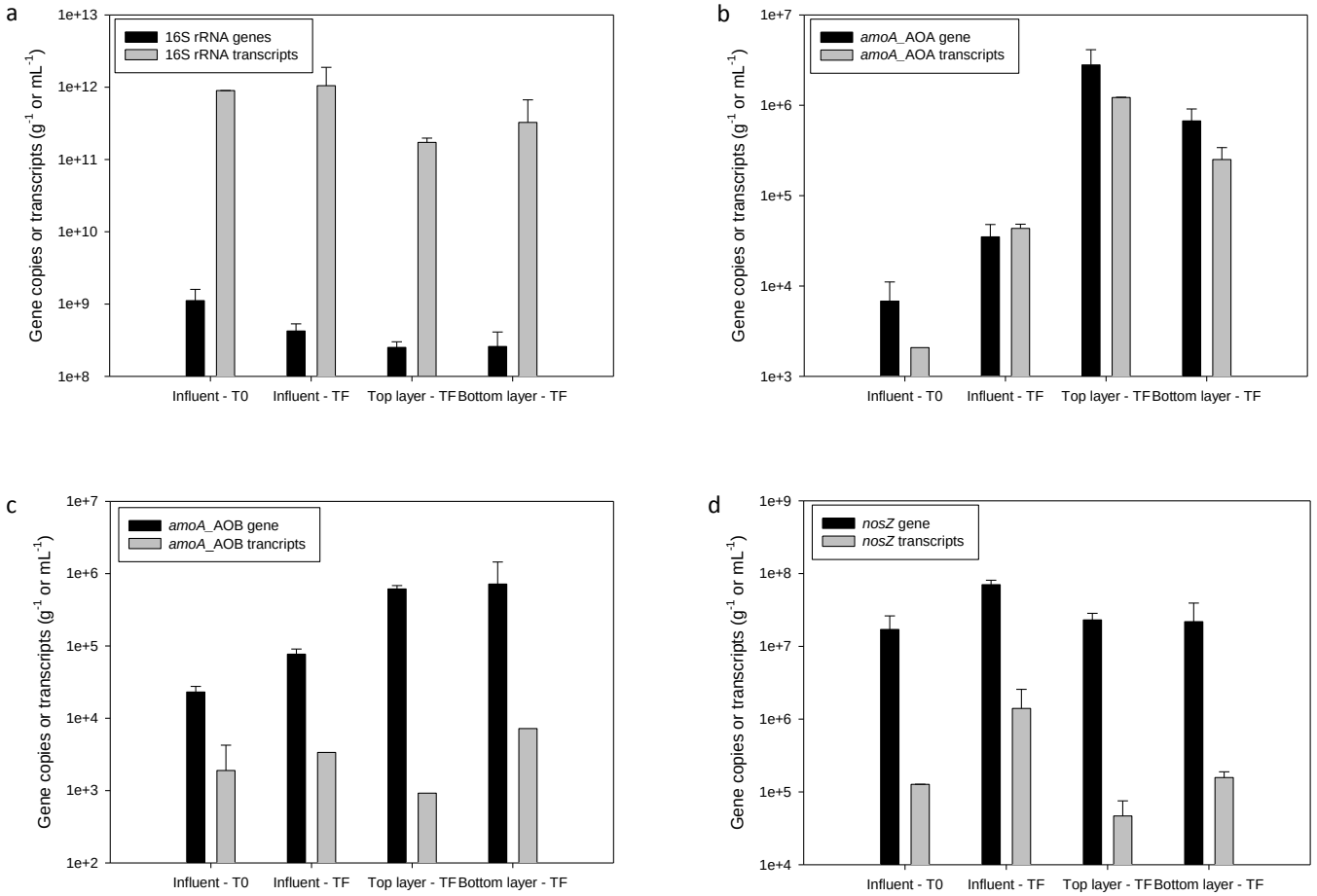

Figure S2. Average and standard deviation of functional genes identified in the unsaturated vertical flow wetland (UVF). (a) Total bacterial population; (b) AOA population; (c) AOB population; (d) Denitrifiers (clade I) gene and transcript counts determined by qPCR. Triplicates were taken from influent and bed material of top (0-15 cm) and bottom (70-80 cm) of UVF wetland at the end of the study (TF).

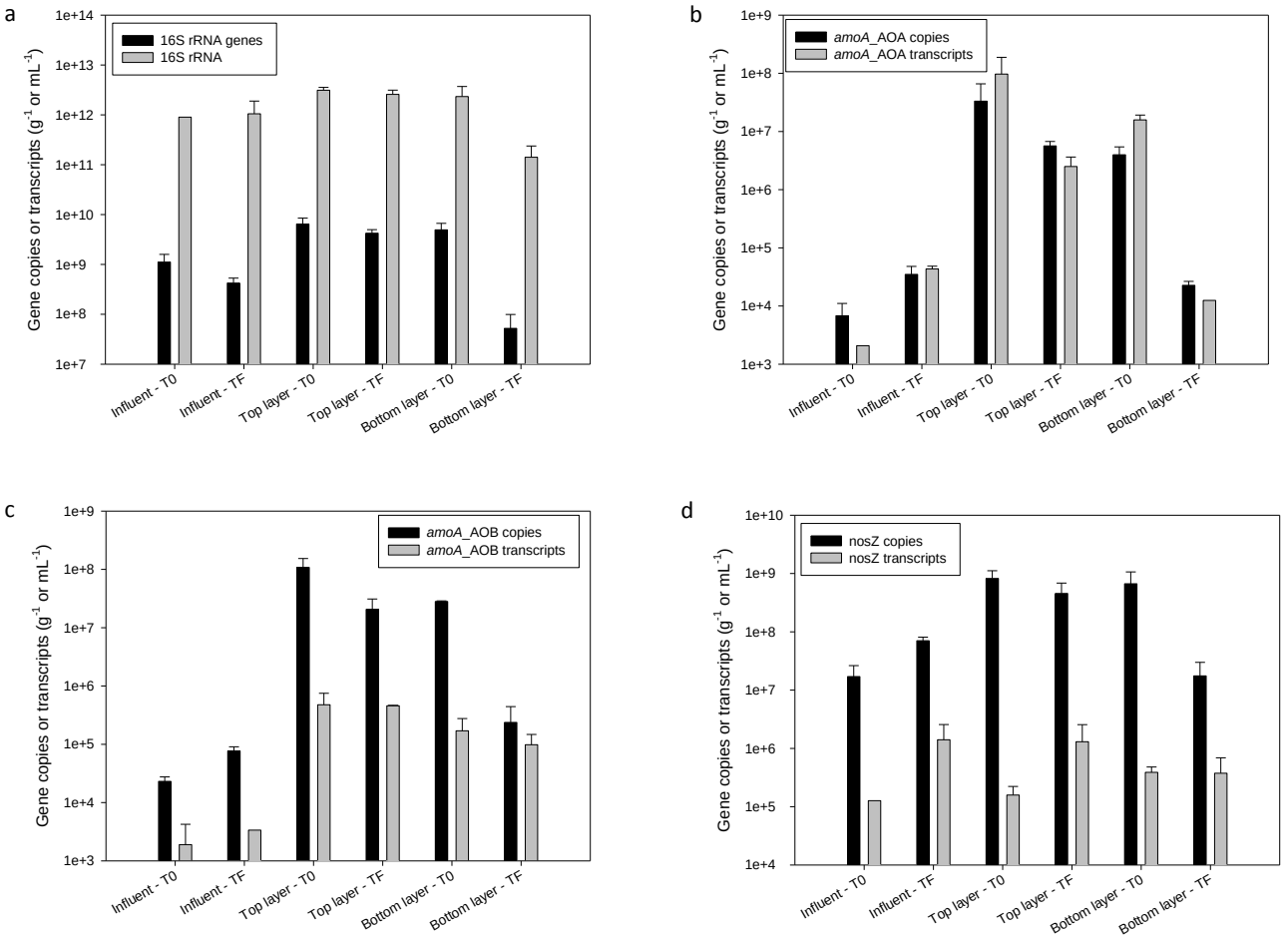

Figure S3. Average and standard deviation of functional genes identified in the partially saturated vertical flow wetland (SVF). (a) Total bacterial population; (b) AOA population; (c) AOB population; (d) Denitrifiers (clade I) of the gene and transcript counts determined by qPCR. Triplicates were taken from influent and bed material of top (0-15 cm) and bottom (70-80 cm) of UVF wetland at the end of the study (TF).

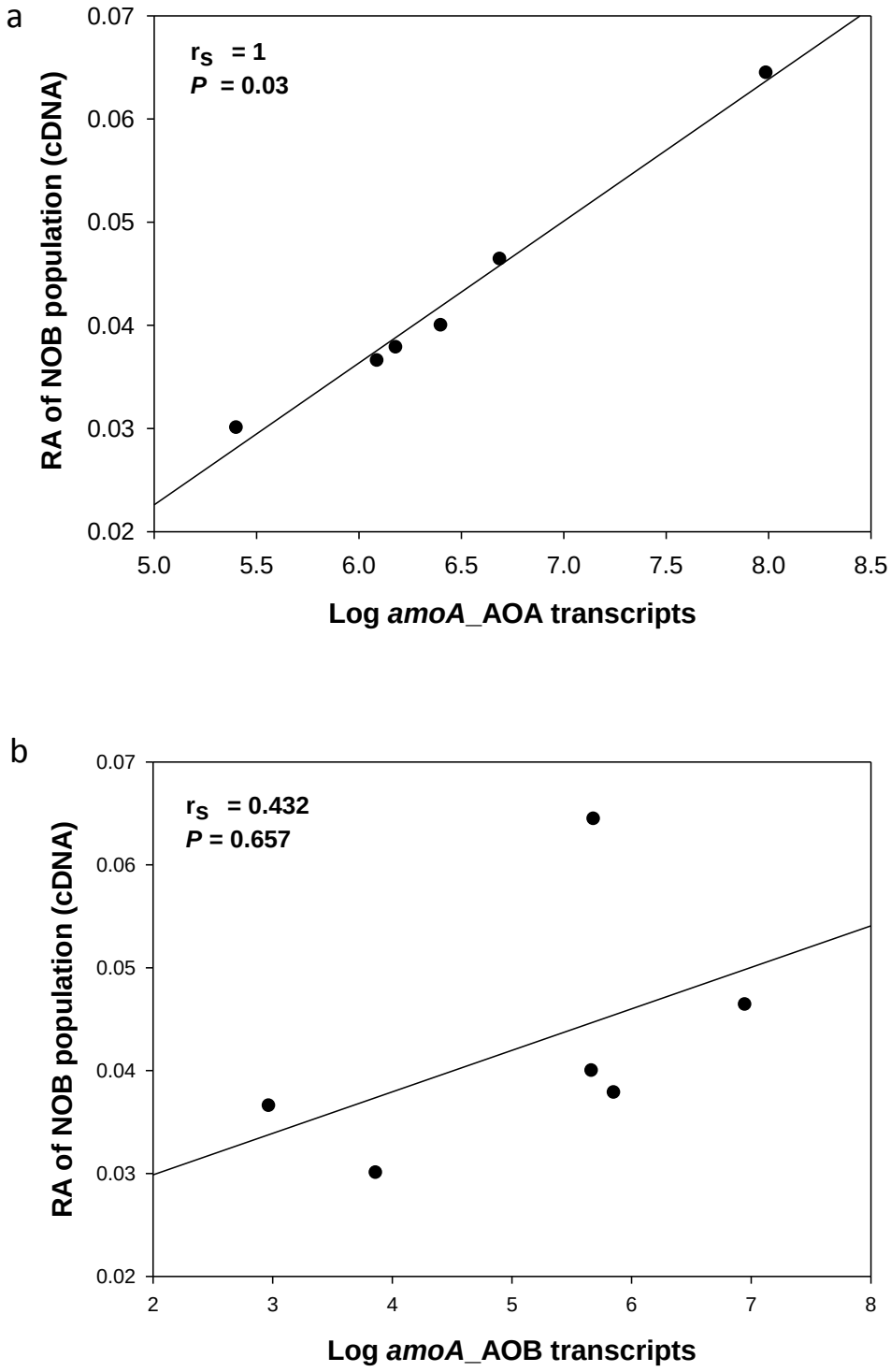

Figure S4. Correlation plots between nitrifying populations. (a) Active AOA population and RA of NOB (both *Nitrobacter* spp. and *Nitrospira* spp.); (b) Active AOB population and RA of NOB (both *Nitrobacter* spp. and *Nitrospira* spp.). Data used in this figure is referred to the starting and ending periods for both wetlands (T0 and TF) and the top and bottom layers of UVF and the top layer of SVF. The qPCR and NGS data of the previous study (Table S1) conducted in the UVF wetland (Pelissari et al., 2017b) was also included.

Table S1. Average of qPCR results (standard deviation) and cDNA-based NGS results, published in Pelissari et al. (2017). Triplicates were sampled in the same layer of the current unsaturated vertical subsurface flow wetland (UVF): in top (0-15 cm) and bottom (70-80 cm) layers at the ending period of the published study.

Parameters for correlations	Top layer (ending period)	Bottom layer (ending period)
*amoA*_ AOA transcripts (g^{-1} of filter media)	$1.51 \cdot 10^6$ ($8.56 \cdot 10^5$)	$4.86 \cdot 10^6$ ($3.50 \cdot 10^6$)
*amoA*_ AOB transcripts (g^{-1} of filter media)	$7.05 \cdot 10^5$ ($8.85 \cdot 10^5$)	$8.81 \cdot 10^6$ ($4.77 \cdot 10^6$)
nosZ transcripts (g^{-1} of filter media)	$9.23 \cdot 10^4$ ($6.18 \cdot 10^4$)	$3.43 \cdot 10^6$ ($1.12 \cdot 10^6$)
Nitrobacter spp. (% Relative abundance; bootstrap value >80%)	3.63	4.18
Nitrospira spp. (% Relative abundance; bootstrap value >80%)	0.16	0.47

Table S2. Relative abundance of nitrite oxidizing bacteria (NOB) identified in top and bottom layers from unsaturated (UVF) and partially saturated vertical (SVF) flow wetlands. Taxonomical assignment (genus level) was performed according to the RDP Bayesian Classifier database with a bootstrap confidence above 80%. These 16Sr RNA-based NGS RA results were used to perform AOP and NOB correlations.

OTUs	Genus	Bootstrap value (RDP)	SVF wetland				UVF wetland	
			Top layer	Bottom layer*	Top layer	Bottom layer*	Top layer	Bottom layer
			Initial Period (T0)		Ending Period (TF)		Ending Period (TF)	
OTU_5	*Nitrobacter*	84%	5.874%	3.495%	1.871%	2.456%	1.002%	0.885%
OTU_2984	*Nitrobacter*	84%	0.015%	0.022%	0.009%	0.003%	0.002%	0.000%
OTU_3407	*Nitrobacter*	82%	0.192%	0.157%	0.056%	0.058%	0.025%	0.016%
OTU_4478	*Nitrobacter*	87%	0.008%	0.003%	0.002%	0.000%	0.000%	0.002%
OTU_4513	*Nitrobacter*	89%	0.003%	0.002%	0.000%	0.000%	0.007%	0.003%
OTU_4614	*Nitrobacter*	82%	0.008%	0.005%	0.003%	0.000%	0.003%	0.003%
OTU_4894	*Nitrobacter*	92%	0.067%	0.052%	0.023%	0.014%	0.008%	0.009%
OTU_5167	*Nitrobacter*	90%	0.005%	0.003%	0.000%	0.000%	0.000%	0.000%
Total Relative abundance (%) of *Nitrobacter* spp.			6.172%	3.739%	1.964%	2.531%	1.048%	0.918%
OTU_7	*Nitrospira*	100%	0.102%	3.933%	0.883%	0.345%	2.059%	1.657%
OTU_73	*Nitrospira*	100%	0.126%	0.605%	0.568%	0.047%	0.172%	0.214%
OTU_190	*Nitrospira*	95%	0.020%	0.017%	0.498%	0.047%	0.160%	0.092%
OTU_491	*Nitrospira*	100%	0.002%	0.007%	0.000%	0.002%	0.109%	0.085%
OTU_1349	*Nitrospira*	100%	0.002%	0.002%	0.002%	0.000%	0.049%	0.002%
OTU_2631	*Nitrospira*	100%	0.000%	0.002%	0.012%	0.000%	0.008%	0.003%
OTU_3396	*Nitrospira*	100%	0.000%	0.000%	0.014%	0.000%	0.002%	0.000%
OTU_3537	*Nitrospira*	100%	0.000%	0.000%	0.012%	0.000%	0.003%	0.000%
OTU_4230	*Nitrospira*	100%	0.000%	0.000%	0.000%	0.002%	0.002%	0.005%
OTU_4298	*Nitrospira*	100%	0.000%	0.003%	0.003%	0.000%	0.000%	0.003%
OTU_5268	*Nitrospira*	100%	0.000%	0.000%	0.000%	0.000%	0.000%	0.006%

Table S2. Relative abundance of nitrite oxidizing bacteria (NOB) identified in top and bottom layers from unsaturated (UVF) and partially saturated vertical (SVF) wetlands. Taxonomical assignment (genus level) was performed according to the RDP Bayesian Classifier database with a bootstrap confidence above 80%. These 16Sr RNA-based NGS RA results were used to perform AOP and NOB correlations. Continuation.

OTUs	Genus	Bootstrap value (RDP)	SVF wetland				UVF wetland	
			Top layer	Bottom layer*	Top layer	Bottom layer*	Top layer	Bottom layer
			Initial Period (T0)		Ending Period (TF)		Ending Period (TF)	
OTU_5535	*Nitrospira*	100%	0.000%	0.005%	0.002%	0.000%	0.003%	0.005%
OTU_5617	*Nitrospira*	100%	0.000%	0.000%	0.007%	0.000%	0.005%	0.002%
OTU_6639	*Nitrospira*	100%	0.000%	0.003%	0.002%	0.000%	0.000%	0.000%
OTU_6642	*Nitrospira*	86%	0.000%	0.000%	0.009%	0.000%	0.000%	0.002%
OTU_6792	*Nitrospira*	100%	0.000%	0.002%	0.000%	0.000%	0.003%	0.003%
OTU_6799	*Nitrospira*	100%	0.000%	0.013%	0.005%	0.000%	0.007%	0.002%
OTU_7475	*Nitrospira*	100%	0.000%	0.005%	0.003%	0.002%	0.000%	0.000%
Total Relative abundance (%) of *Nitrospira* spp.			0.251%	4.596%	2.021%	0.443%	2.583%	2.079%
Total Relative abundance (%) of total NOB			6.42%	8.335%	3.985%	2.974%	3.631%	2.997%

*Relative abundance values of SVF wetland from bottom layer (T0 and TF) were not used for correlations.

Table S3. Taxonomic affiliation of the most predominant bacterial OTUs (above 1% of the RA at least one sample). Taxonomical assignment (taxon levels) was performed according to the RDP Bayesian Classifier database with a bootstrap confidence above 80%.

OTUs	Phylum	Class	Order	Family	Genus
OTU_1	*Proteobacteria*	*Gammaproteobacteria*	*Pseudomonadales*	*Pseudomonadaceae*	*Pseudomonas*
OTU_2	*Firmicutes*	*Clostridia*	*Clostridiales*	*Peptostreptococcaceae*	*Clostridium XI*
OTU_3	*Proteobacteria*	*Epsilonproteobacteria*	*Campylobacterales*	*Campylobacteraceae*	*Arcobacter*
OTU_4	*Actinobacteria*	*Actinobacteria*	*Actinomycetales*	*Streptomycineae*	*Streptomyces*
OTU_5	*Proteobacteria*	*Alphaproteobacteria*	*Rhizobiales*	*Bradyrhizobiaceae*	*Nitrobacter*
OTU_6	*Proteobacteria*	*Alphaproteobacteria*	*Rhizobiales*	*Hyphomicrobiaceae*	*Hyphomicrobium*
OTU_7	*Nitrospirae*	*Nitrospira*	*Nitrospirales*	*Nitrospiraceae*	*Nitrospira*
OTU_8	*Proteobacteria*	*Alphaproteobacteria*	*Rhodobacterales*	*Rhodobacteraceae*	Unclassified
OTU_9	*Planctomycetes*	*Planctomycetia*	*Planctomycetales*	*Planctomycetaceae*	Unclassified
OTU_10	*Proteobacteria*	*Betaproteobacteria*	*Rhodocyclales*	*Rhodocyclaceae*	*Dechloromonas*
OTU_11	*Proteobacteria*	*Deltaproteobacteria*	*Myxococcales*	*Sorangiineae*	Unclassified
OTU_12	*Chloroflexi*	*Ktedonobacteria*	*Ktedonobacterales*	Unclassified	
OTU_13	*Proteobacteria*	*Deltaproteobacteria*	*Myxococcales*	*Sorangiineae*	*Unclassified*
OTU_14	*Proteobacteria*	*Betaproteobacteria*	*Rhodocyclales*	*Rhodocyclaceae*	*Dechloromonas*
OTU_15	*Bacteroidetes*	*Bacteroidetes_incertae_sedis*	*Ohtaekwangia*	Unclassified	
OTU_16	*Proteobacteria*	*Gammaproteobacteria*	*Pseudomonadales*	*Pseudomonadaceae*	*Pseudomonas*
OTU_17	*Planctomycetes*	*Planctomycetia*	*Planctomycetales*	*Planctomycetaceae*	*Telmatocola*
OTU_18	*Acidobacteria*	*Holophagae*	*Holophagales*	*Holophagaceae*	*Geothrix*
OTU_20	*Proteobacteria*	*Gammaproteobacteria*	*Acidithiobacillales*	*Acidithiobacillaceae*	*Acidithiobacillus*
OTU_21	*Proteobacteria*	*Betaproteobacteria*	Unclassified		
OTU_22	*Proteobacteria*	*Betaproteobacteria*	Unclassified		
OTU_23	*Proteobacteria*	*Betaproteobacteria*	*Burkholderiales*	*Comamonadaceae*	*Acidovorax*
OTU_24	*Firmicutes*	*Clostridia*	*Clostridiales*	*Clostridiaceae 1*	*Clostridium sensu stricto*
OTU_26	*Bacteroidetes*	*Flavobacteriia*	*Flavobacteriales*	*Flavobacteriaceae*	*Cloacibacterium*
OTU_27	*Acidobacteria*	*Acidobacteria_Gp4*	*Gp4*	*Unclassified*	

Table S3. Taxonomic affiliation of the most predominant bacterial OTUs (above 1% of the RA at least one sample). Taxonomical assignment (taxon levels) was performed according to the RDP Bayesian Classifier database with a bootstrap confidence above 80%. Continuation.

OTUs	Phylum	Class	Order	Family	Genus
OTU_28	*Chloroflexi*	*Ktedonobacteria*	*Ktedonobacterales*	*Unclassified*	
OTU_30	*Proteobacteria*	*Deltaproteobacteria*	*Myxococcales*	*Sorangiineae*	
OTU_32	*Firmicutes*	*Bacilli*	*Bacillales*	*Bacillaceae 1*	*Bacillus*
OTU_33	Unclassified				
OTU_35	*Firmicutes*	*Bacilli*	*Lactobacillales*	*Carnobacteriaceae*	*Trichococcus*
OTU_37	*Acidobacteria*	*Acidobacteria_Gp4*	*Gp4*	*Unclassified*	
OTU_39	*Actinobacteria*	*Actinobacteria*	*Actinomycetales*	*Kineosporiineae*	*Angustibacter*
OTU_40	*Bacteroidetes*	*Flavobacteriia*	*Flavobacteriales*	*Flavobacteriaceae*	*Flavobacterium*
OTU_41	*Proteobacteria*	*Epsilonproteobacteria*	Unclassified		
OTU_47	*Proteobacteria*	*Betaproteobacteria*	Unclassified		
OTU_50	*Actinobacteria*	*Actinobacteria*	*Rubrobacteridae*	*Solirubrobacterales*	Unclassified
OTU_51	*Proteobacteria*	*Betaproteobacteria*	*Rhodocyclales*	*Rhodocyclaceae*	*Thauera*
OTU_52	*Proteobacteria*	*Gammaproteobacteria*	*Xanthomonadales*	*Xanthomonadaceae*	*Dyella*
OTU_59	*Proteobacteria*	Unclassified			
OTU_62	*Proteobacteria*	*Deltaproteobacteria*	*Myxococcales*	*Sorangiineae*	Unclassified
OTU_63	Unclassifed				
OTU_70	*Actinobacteria*	*Actinobacteria*	*Actinomycetales*	*Corynebacterineae*	*Mycobacterium*
OTU_124	*Proteobacteria*	*Betaproteobacteria*	*Hydrogenophilales*	*Hydrogenophilaceae*	*Thiobacillus*
OTU_191	*Actinobacteria*	*Actinobacteria*	*Actinomycetales*	*Micrococcineae*	Unclassified

Table S4. Taxonomic affiliation of the most predominant archaeal OTUs (above 1% of the RA at least one sample). Taxonomical assignment (taxon levels) was performed according to the RDP Bayesian Classifier database with a bootstrap confidence above 80%.

OTUs	Phylum	Class	Order	Family	Genus
OTU_1	*Euryarchaeota*	*Methanomicrobia*	*Methanosarcinales*	*Methanotrichaceae*	*Methanothrix*
OTU_2	*Thaumarchaeota*	*Nitrososphaeria*[*]	*Nitrososphaerales*	*Nitrososphaeraceae*	*Nitrososphaera*
OTU_3	*Euryarchaeota*	*Methanobacteria*	*Methanobacteriales*	*Methanobacteriaceae*	*Methanobrevibacter*
OTU_7	*Euryarchaeota*	*Methanobacteria*	*Methanobacteriales*	*Methanobacteriaceae*	*Methanobrevibacter*
OTU_11	*Thaumarchaeota*	*Nitrososphaeria*	*Nitrosopumilales*	*Nitrosopumilaceae*	*Nitrosopumilus*
OTU_16	*Euryarchaeota*	*Methanobacteria*	*Methanobacteriales*	*Methanobacteriaceae*	*Methanobacterium*
OTU_18	*Euryarchaeota*	*Methanobacteria*	*Methanobacteriales*	*Methanobacteriaceae*	*Methanosphaera*
OTU_20	*Thaumarchaeota*	*Nitrososphaeria*	*Nitrososphaerales*	*Nitrososphaeraceae*	*Nitrososphaera*
OTU_21	*Thaumarchaeota*	*Nitrososphaeria*[*]	*Nitrosopumilales*	*Nitrosopumilaceae*	*Nitrosopumilus*
OTU_26	*Euryarchaeota*	*Methanomicrobia*	*Methanomicrobiales*	*Methanoregulaceae*	*Methanoregula*
OTU_32	*Euryarchaeota*	*Methanomicrobia*	*Methanomicrobiales*	*Methanospirillaceae*	*Methanospirillum*
OTU_33	*Euryarchaeota*	*Methanomicrobia*	*Methanosarcinales*	*Methanosarcinaceae*	*Methanomethylovorans*
OTU_339	*Euryarchaeota*	*Methanomicrobia*	*Methanosarcinales*	*Methanotrichaceae*	*Methanothrix*
OTU_697	*Euryarchaeota*	*Methanomicrobia*	*Methanosarcinales*	*Methanotrichaceae*	*Methanothrix*
OTU_1993	*Thaumarchaeota*	*Nitrososphaeria*	*Nitrososphaerales*	*Nitrososphaeraceae*	*Nitrososphaera*

[*]Taxonomy affiliation proposed by Qin et al. (2017).

Table S5. Relative abundance of ammonia oxidizing bacteria (AOB) identified in top and bottom layers from unsaturated (UVF) and partially saturated vertical (SVF) flow wetlands. Taxonomical assignment (family level) was performed according to the RDP Bayesian Classifier database with a bootstrap confidence above 80%.

			SVF wetland				UVF wetland	
OTUs	Family	Bootstrap value (RDP)	Top layer	Bottom layer	Top layer	Bottom layer	Top layer	Bottom layer
			Initial Period (T0)		Ending Period (TF)		Ending Period (TF)	
OTU_65	*Nitrosomonadaceae*	100%	0.477%	0.325%	0.126%	0.181%	0.024%	0.017%
OTU_1404	*Nitrosomonadaceae*	97%	0.002%	0.007%	0.044%	0.003%	0.000%	0.000%
OTU_1695	*Nitrosomonadaceae*	85%	0.002%	0.015%	0.023%	0.000%	0.000%	0.000%
OTU_2512	*Nitrosomonadaceae*	98%	0.000%	0.030%	0.007%	0.000%	0.000%	0.000%
OTU_4243	*Nitrosomonadaceae*	98%	0.013%	0.010%	0.003%	0.000%	0.000%	0.000%
OTU_5433	*Nitrosomonadaceae*	98%	0.008%	0.002%	0.002%	0.000%	0.000%	0.000%
OTU_5531	*Nitrosomonadaceae*	91%	0.003%	0.000%	0.000%	0.000%	0.000%	0.008%
OTU_6002	*Nitrosomonadaceae*	96%	0.000%	0.000%	0.003%	0.002%	0.000%	0.000%
OTU_6518	*Nitrosomonadaceae*	89%	0.003%	0.000%	0.000%	0.000%	0.000%	0.003%
Total Relative abundance (%) *Nitrosomonadaceae*			0.508%	0.389%	0.208%	0.186%	0.024%	0.028%

REFERENCES

Calderer, M., Martí, V., de Pablo, J., Guivernau, G., Prenafeta-Boldú, F.X., Viñas, M., 2014. Effects of enhanced denitrification on hydrodynamics and microbial community structure in a soil column system. Chemosphere 111, 112–119.

Caporaso, J.G., K. Bittinger, F.D. Bushman, T.Z. DeSantis, G.L. Andersen, R. Knight., 2010b. PyNAST: A flexible tool for aligning sequences to a template alignment. Bioinformatics. 26, 266–267.

Caporaso, J.G., Kuczynski, J., Stombaugh, J., Bittinger, K., Bushman, F.D., Costello, E.K., 2010a. QIIME allows analysis of high-throughput community sequencing data. Nat. Methods. 7, 335–336.

De Santis, T.Z., Hugenholtz, P., Larsen, N., Rojas, M., Brodie, E.L., Keller, K., Huber, T., Dalevi, D., Hu, P., Andersen, G.L., 2006. Greengenes, a chimera-checked 16 S rRNA gene database and workbench compatible with ARB. Appl. Environ. Microbiol. 72, 5069–5072.

Haas, B.J., Gevers, D., Earl, A.M., Feldgarden, M., Ward, D. V, Giannoukos, G., Ciulla, D., Tabbaa, D., Highlander, S.K., Desantis, T.Z., Sodergren, E., Methe, B., Human, T., Consortium, M., Petrosino, J.F., Knight, R., Birren, B.W. 2011. Chimeric 16S rRNA sequence formation and detection in Sanger and 454-pyrosequenced PCR amplicons.Genome Res. 494–504.

Pelissari, C., Guivernau, M., Viñas, M., Silva, S.S., García, J., Sezerino, P.H. Ávila, C., 2017. Unraveling the active microbial populations involved in nitrogen utilization in a vertical subsurface flow constructed wetland treating urban wastewater. Sci. Total Environ. 584-585, 642-650.

Prenafeta-Boldú, F. X., Guivernau, M., Gallastegui, G., Viñas, M., de Hoog, G. S., Elías, A., 2012. Fungal/bacterial interactions during the biodegradation of TEX hydrocarbons (toluene, ethylbenzene and p-xylene) in gas biofilters operated under xerophilic conditions. FEMS Microbiol. Ecol. 80, 722–734.

Qin, W., Heal, K., Ramdasi, R., Kobelt, J., Martens-Habbena, W., Bertagnolli, A., Amin, S., Walker, C., Urakawa, H., Könneke, M., Devol, A., Moffett, J., Armbrust, E., Jensen, G., Ingalls, A., Stahl, D., 2017.*Nitrosopumilus maritimus* gen. nov., sp. nov., *Nitrosopumilus cobalaminigenes* sp. nov., *Nitrosopumilus oxyclinae* sp. nov., and *Nitrosopumilus ureiphilus* sp. nov., four marine ammonia-oxidizing archaea of the phylum *Thaumarchaeota.* Int J Syst Evol Microbiol. 16.

Reeder, J., Knight, R., 2010. Rapidly denoising pyrosequencing amplicon reads by exploiting rank-abundance distributions. Nature Methodos. 2, 668–669.

Rotthauwe, J.H., Witzel, K.P., Liesack, W., 1997. The ammonia monooxygenase struc- tural gene amoA as a functional marker: molecular fine-scale analysis of natural ammonia-oxidizing populations. Appl. Environ. Microbiol. 63, 4704–4712.

454 wastewater had relatively low NH_4-N concentrations (19 ± 4 mg L^{-1}), which could
455 presumably have favored the AOA community at expenses of AOB (Fig. 4**,** S2
456 and S3) in aerobic layers. Moreover, these results are also in accordance with a
457 recent study of wetland paddy fields that observed that in microaerophilic
458 conditions AOA have greater advantage over AOB, depending on
459 physicochemical properties of the media, including pH and redox conditions
460 (Wang et al., 2015). Stempfhuber et al. (2015) in an unfertilized grassland soil
461 (where oxygen played an important role in substrate limiting conditions) found the
462 same trend. Nitrification was predominantly accomplished by AOA and *Nitrospira,*
463 being this co-occurrence in a limited spatial scale (Aug-Oct). Presumably, a
464 mixotrophic metabolism of AOA and *Nitrospira* could increment the
465 competitiveness over their counterparts by providing a growth advantage under
466 substrate limiting conditions (Lehtovirta-Morley et al., 2014).

467 With regard to the denitrifying population, RNA-based assays showed that not all
468 denitrifiers from clade I had the optimal conditions to be active since the *nosZ*
469 gene abundance was always greater than the transcripts (Fig. S2 and S3). Taking
470 into account *nosZ* ratios (Fig. 4), denitrifiers exhibited statistical differences ($P <$
471 0.05) in the bottom layer of the SVF wetland at final period (TF). Moreover, *nosZ*
472 gene expression on the biofilms was similar to *amoA* transcripts (both AOA and
473 AOB), which confirms the occurrence of a simultaneous nitrification and complete
474 denitrification process in the SVF wetland with no transient accumulation of NO_x-
475 N. It is important to mention that this active denitrification could be preventing the
476 nitric oxide (NO) accumulation, thus conditioning the metabolism of AOA due to
477 their NO dependence during the ammonia oxidizing process (Kozlowski et al.,
478 2016). On the other hand, in the UVF unit the lower presence and activity of

denitrifiers linked with the highest AOA activity were also in agreement with the build-up of NO_x-N.

In conclusion, denitrifying populations took an active role under more reductive conditions and organic carbon availability (Fig. S1). Interestingly, NGS data revealed that active families of potential denitrifiers could belong to *nosZ* clade I and clade II at a similar proportion (Domeignoz-Horta et al., 2016; Jones et al., 2013; Samad et al., 2016; Sandford et al., 2012; Yoon et al., 2016). Although N_2O emissions have not been monitored in the present study, combining data from online N_2O sensors with the functional expression of NDN-based genes could contribute to the implementation of more sustainable nitrogen removal technologies in urban wastewater treatment (Andalib et al., 2018).

3.2.4 Potential interactions among active nitrifying populations

Unraveling the interactions between different microbial species in biofilms is a challenge, especially when biofilms are attached to the bed media from several biotechnological processes. This is the main reason why microbe-microbe interactions among nitrifiers in CW have not been completely revealed yet.

In this study, relevant nitrifying microbial dynamics were observed when oxic and/or microaerophilic conditions prevailed in the VF units, when considering *amoA* transcripts from AOP and the RA of NOB (Fig. 5 and S4). Each pair of variables, on which Spearman's ranked correlation test was performed to study their relationship, counted on six experimental points: from top and bottom layers of the UVF wetland of the current and the previous study (Pelissari et al., 2017b - Table S1), and from the top layer of the SVF wetland, at the initial (T0) and final

(TF) period of the present study. The bottom layer of the SVF was excluded due to the negative redox conditions and the complete different behavior.

With regard to the NOB population (Fig. 5a), a negative correlation, was found between RA of *Nitrospira* and *Nitrobacter* (r_s = -0.77; *P* = 0.10). As mentioned above, *K/r* strategy linked with oxygen and nitrite concentrations under certain physicochemical conditions could directly affect NOB dynamics.

Looking at *amoA* transcripts of the AOP population, a positive correlation was observed between the logarithm of the number of AOA transcripts and the RA of *Nitrobacter* (r_s = 0.94; *P* = 0.03) (Fig. 5b). This possible symbiosis could be explained by the fact that NOB can produce nitric oxide (NO), a key intermediate in AOA ammonia-oxidizing pathway (Kozlowski et al., 2016) and besides, could act as an electron flux regulator in *Nitrobacter* (Starkenburg et al., 2008). In fact, metabolically active NOB in oxygenic layers showed a higher positive correlation (r_s = 1; *P* = 0.03) with the AOA activity, while the correlation with AOB was lower (r_s = 0.43; *P* = 0.66) (Fig. S4).

On the other hand, Fig. 5c shows a negative correlation between the logarithm of the number of AOB transcripts and the RA of *Nitrospira* (r_s = -0.83; *P* = 0.06) inside the biofilm aggregates of oxygenic/microaerophilic layers. This behavior elucidates a potential comammox activity by some *Nitrospira* members, due to the discovery of their capacity to catalyze the complete nitrification (Daims et al., 2015). However, current physicochemical and microbial data are not sufficient to confirm this hypothesis. Despite this fact, NGS data revealed a clear competence between *Nitrospira* and AOB in a microaerophilic ambient in substrate limiting conditions. Contrarily, *Nitrospira* could not outcompete in the same way with the AOA population, presumably owing to the preference for relatively low ammonia

concentrations. Daims et al. (2016) postulated that, in habitats where the *Nitrospira* population is greater than AOP communities, there could be an indication of the comammox process. In the current study, *Nitrospira* was detected by high-throughput sequencing but not assessed by qPCR and therefore quantitative amounts of *Nitrospira* could not be revealed. It is important to note that the AOB population by NGS data was always ten-fold lower than the percentage of *Nitrospira*. Nonetheless, we cannot conclude that comammox process prevails in aerobic bed media because *amoA*_AOA transcripts were always one or two orders greater than AOB. Finally, it is noteworthy to mention that through the comammox process *Nitrospira* lacks the capacity to produce N_2O (Palomo et al., 2016). Thus, the promotion of its enrichment in CW could improve the NDN process, subsequently diminishing greenhouse gas emissions.

CONCLUSIONS

Based on different nitrogen transformations linked with microbial community dynamics within a conventional unsaturated vertical (UVF) and a partially saturated vertical (SVF) flow CW operated in parallel for half a year, main conclusions were as follows:

- COD and NH_4-N load removal were similar in both CW. However, the SVF wetland presented a significant higher TN load removal.
- Nitrification processes predominated within the UVF wetland due to the higher occurrence of oxidative conditions. Oppositely, the denitrification potential of the SVF wetland was higher due to the partial saturation of the filter bed, showing no NO_x-N accumulation.

- The occurrence of simultaneous NDN process in the SVF wetland was boosted due to higher availability of organic carbon linked with reductive conditions.
- AOA/AOB/NOB dynamics, potentially related to '*nitrification-aggregates*', were observed in the upper oxygenic layers of both CW as part of bed biofilms.
- AOA and *Nitrobacter* showed a positive correlation outcompeting their counterparts. *Nitrospira* is proposed to act as comammox organism overcoming the AOB population in the oxic layers.
- Due to nitrifier-denitrifying capability, AOB were more actively enriched than AOA in hypoxic layer of the SVF wetland, concomitantly with total active denitrifying community.
- AOA clearly exerted a key role, being the most active and predominant AOP population in both wetlands.
- Findings demonstrated that different CW configurations directly affect the TN removal efficiency, as well as the active microbial community established in the biofilms, being RNA studies a suitable NDN sensor.

ACKNOWLEDGEMENTS

C. A. acknowledges a postdoctoral grant (FJCI-2014-22245) from the Spanish Ministry of Economy and Competitiveness (Plan Nacional de I + D + i 2008–2011, Subprograma Juan de la Cierva (JDC) 2014). C.P. acknowledges a sandwich doctorate grant from the Coordination for the Improvement of Higher Level (CAPES PDSE 99999.006475/2015-09). This research was also supported by

the CERCA Programme / Generalitat de Catalunya. The authors are thankful to Dr. Francesc Prenafeta-Boldú for reviewing the manuscript, to Noemie Devesa for assistance during sampling and analysis of water quality parameters, and to Nuria Roca for the support in molecular laboratory work.

REFERENCES

Álvarez, J.A., Ávila, C., Otter, P., Kilian, R., Istenič, D., Rolletschek, M., Molle, P., Khalil, N., Ameršek, I., Mishra, V.K., Jorgensen, C., Garfi, A., Carvalho, P., Brix, H., Arias, C.A., 2017. Constructed wetlands and solar-driven disinfection technologies for sustainable wastewater treatment and reclamation in rural India: SWINGS project. Water Sci. Technol. 76, 1474–1489.

Andalib, M., Taher, E., Donohue, J., Ledwell, S., Andersen, M. H., Sangrey, K., 2018. Correlation between nitrous oxide (N_2O) emission and carbon to nitrogen (COD/N) ratio in denitrification process: a mitigation strategy to decrease greenhouse gas emission and cost of operation. Water Sci.Technol. 77, 426–438.

APHA, 2012. Standard Methods for the Examination of Water and Wastewater. 22th ed. American Public Health Association, Washington, DC, USA.

Austin, D., Wolf, L., Strous, M., 2006. Mass transport and microbiological mechanisms of nitrification and denitrification in tidal flow constructed wetland systems. In: 10th International Conference on Wetland Systems for Water Pollution Control, Lisbon, Portugal, 209–216.

Ávila, C., García, J., 2015. Pharmaceuticals and personal care products (PPCPs) in the environment and their removal from wastewater through constructed wetlands. In: Zeng, E. (Ed.), Comprehensive Analytical Chemistry; Persistent Organic Pollutants: Analytical Techniques, Environmental Fate and Biological Effects vol. 67. Elsevier, pp. 199-244 (chapter 6).

602 Ávila, C., García, J., Garfí, M., 2016. Influence of hydraulic loading rate, simulated
603 storm events and seasonality on the treatment performance of an experimental
604 three-stage hybrid constructed wetland system. Ecol. Eng. 87, 324–332.

605 Ávila, C., Pelissari, C., Sgroi, M., Roccaro, P., Sezerino, P.H., García, J., 2017.
606 Enhancement of total nitrogen through effluent recirculation and fate of PPCPs in
607 a hybrid constructed wetland system treating urban wastewater. Sci. Total
608 Environ. 584-585, 414–425.

609 Button, M., Rodriguez, M., Brisson, J., Weber, K.P., 2016. Use of two spatially
610 separated plant species alters microbial community function in horizontal
611 subsurface flow constructed wetlands. Ecol. Eng. 92, 18–27.

612 Brenzinger, K., Dörsch, P., Braker, G., 2015. pH-driven shifts in overall and
613 transcriptionally active denitrifiers control gaseous product stoichiometry in
614 growth experiments with extracted bacteria from soil. Front. Microbiol. 6, 1–11.

615 Chen, Y., Wen, Y., Zhou, Q., Huang, J., Vymazal, J., Kuschk, P., 2016. Sulfate
616 removal and sulfur transformation in constructed wetlands : The roles of fi lling
617 material and plant biomass. Water Res. *102*, 572–581.

618 Cydzik-Kwiatkowska, A., Zielińska, M., 2016. Bacterial Communities in Full-Scale
619 Wastewater Treatment Systems. World J. Microbiol. Biotechnol. 32–66.

620 Daims, H., Elena, V., Palatinszky, M., Vierheilig, J., Bulaev, A., Kirkegaard, R.H.,
621 Bergen, M. Von, Rattei, T., 2015. Complete nitrification by Nitrospira bacteria.
622 Nature. 528, 504–509.

623 Daims, H., Lucker, S., Wagner, M., 2016. A new perspective on microbes
624 formerly known as nitrite-oxidizing bacteria. Trends in Microbiol. 24, 699–712.

625 Dong, Z., Sun, T., 2007. A potential new process for improving nitrogen removal
626 in constructed wetlands—Promoting coexistence of partial-nitrification and
627 ANAMMOX. Ecol. Eng. 31, 69–78.

628 Domeignoz-Horta, L.A., Putz, M., Spor, A., Bru, D., Breuil, M.C., Hallin, S.,
629 Philippot, L., 2016. Non-denitrifying nitrous oxide-reducing bacteria - An effective
630 N_2O sink in soil. Soil Biology and Biochem. 103, 376–379.

631 Fan, L. F., Chen, H. J., Hsieh, H. L., Lin, H. J., Tang, S. L., 2016. Comparing
632 abundance, composition and environmental influences on prokaryotic ammonia
633 oxidizers in two subtropical constructed wetlands. Ecol. Eng. 90, 336–346.

634 Faulwetter, J.L., Gagnon, V., Sundberg, C., Chazarenc, F., Burr, M.D., Brisson,
635 J., Camper, A.K., Stein, O.R., 2009. Microbial processes influencing performance
636 of treatment wetlands: A review. Ecol. Eng. 35, 987–1004.

637 Flemming, H., Wingender, J., Szewzyk, U., Steinberg, P., Rice, A.S., Kjelleberg,
638 S., 2016. Biofilms: an emergent form of bacterial life. Nature Rev. Microbiol. 14, 563–
639 575.

640 Foladori, P., Ruaben, J., Ortigara, A.R.C., 2013. Recirculation or artificial aeration
641 in vertical flow constructed wetlands: a comparative study for treating high load
642 wastewater. Bioresour. Technol. 149, 398–405.

643 Guittonny-Philippe, A., Masotti, M., Höhener, P., Boudenne, J., Viglione, J.,
644 Laffont-Schwob, I., 2014. Constructed wetlands to reduce metal pollution from

645 industrial catchments in aquatic Mediterranean ecosystems: A review to
646 overcome obstacles and suggest potential solutions. Env. Inter. 64, 1–16.

647 Hu, Y., He, F., Ma, L., Zhang, Y., Wu, Z., 2016. Microbial nitrogen removal
648 pathways in integrated vertical-flow constructed wetland systems. Bioresour.
649 Technol. 207, 339–345.

650 Hu, Y., Zhao, Y., Rymszewicz, A., 2014. Robust biological nitrogen removal by
651 creating multiple tides in a single bed tidal flow constructed wetland. Sci. Total
652 Environ. 470-471, 1197–1204.

653 Huang, M., Wang, Z., Qi, R., 2017. Enhancement of the complete autotrophic
654 nitrogen removal over nitrite process in a modified single-stage subsurface
655 vertical flow constructed wetland: Effect of saturated zone depth. Bioresour.
656 Technol. 233, 191–199.

657 Huang, Z., Gedalanga, P.B., Asvapathanagul, P., Olson, B.H., 2010. Influence of
658 physicochemical and operational parameters on *Nitrobacter* and *Nitrospira*
659 communities in an aerobic activated sludge bioreactor. Water Res. 44, 4351–
660 4358.

661 Jones, C.M., Graf, R.H.D., Bru, D., Philippot, L., Hallin, S., 2013. The
662 unaccounted yet abundant nitrous oxide-reducing microbial community: a
663 potential nitrous oxide sink. ISME J.7, 417–426.

664 Kadlec, R.H., Wallace, S.D., 2009. Treatment Wetlands, Treatment Wetlands,
665 Second Edition

666 Koch, H., Lücker, S., Albertsen, M., Kitzinger, K., Herbold, C., Spieck, E., 2015.

667 Expanded metabolic versatility of ubiquitous nitrite-oxidizing bacteria from the
668 genus *Nitrospira*. Proc Natl Acad Sci U S A.112, 11371–11376.

669 Kozlowski, J.A., Stieglmeier, M., Schleper, C., Klotz, M.G., Stein, L.Y., 2016.
670 Pathways and key intermediates required for obligate aerobic ammonia-
671 dependent chemolithotrophy in bacteria and thaumarchaeota. The Multiplic. J.
672 Microbial Ecol.10, 1836–1845.

673 Lehtovirta-morley, L.E., Ge, C., Ross, J., Yao, H., Nicol, G.W., Prosser, J.I., 2014.
674 Characterization of terrestrial acidophilic archaeal ammonia oxidizers and their
675 inhibition and stimulation by organic compounds. FEMS Microb.Ecol. 89, 542–
676 552.

677 Limpiyakorn, T., Sonthiphand, P., Rongsayamanont, C., Polprasert, C., 2011.
678 Abundance of amoA genes of ammonia-oxidizing archaea and bacteria in
679 activated sludge of full-scale wastewater treatment plants. Bioresour. Technol.
680 102, 3694–3701.

681 Maixner, F., Noguera, D.R., Anneser, B., Stoecker, K., Wegl, G., Wagner, M.,
682 Daims, H., 2006. Nitrite concentration influences the population structure of
683 *Nitrospira*-like bacteria. Environ. Microbiol. 8, 1487–1495.

684 Nivala, J., Headley, T., Wallace, S., Bernhard, K., Brix, H., Van Afferden, M.,
685 Müller, R.A., 2013. Comparative analysis of constructed wetlands: The design
686 and construction of the ecotechnology research facility in Langenreichenbach,
687 Germany. Ecol. Eng. 61, 527–543.

688 Orellana, L.H., Rodriguez-R., L.M., Higgins, S., Chee-Sanford, J.C., Sanford, R.,
689 Ritalahti, K., Löffler, F.E., Konstantinidis, K.T., 2014. Detecting nitrous oxide
690 reductase (nosZ) genes in soil metagenomes: method development and
691 implications for the nitrogen cycle. mBio. 5, 1193 –14.

692 Palomo, A., Fowler, S.J., Rasmussen, S., Sicheritz-Pontén, T., Smets, B.F.,
693 2016. Metagenomic analysis of rapid gravity sand filter microbial communities
694 suggests novel physiology of *Nitrospira* spp. ISME J. 10, 2569–2581.

695 Palomo, A., Smets, B.F., Sicheritz-Pontén, T., Rasmussen, S., Baelum, J., 2017.
696 Discovery and description of complete ammonium oxidizers in groundwater-fed
697 rapid sand filters. Kgs. Lyngby: Department of Environmental Engineering,
698 Technical University of Denmark (DTU). At:
699 https://pdfs.semanticscholar.org/1b68/377eef403ff823294307c1753a27d1cbf5d
700 0.pdf accessed on Sep 10th 2017.

701 Pelissari, C., Ávila, C., Maria, C., García, J., Dultra, R., Armas, D., Sezerino, P.H.,
702 2017a. Nitrogen transforming bacteria within a full-scale partially saturated
703 vertical subsurface flow constructed wetland treating urban wastewater. Sci.
704 Total Environ. 574, 390–399.

705 Pelissari, C., Guivernau, M., Viñas, M., Silva, S.S., García, J., Sezerino, P.H.
706 Ávila, C., 2017b. Unraveling the active microbial populations involved in nitrogen
707 utilization in a vertical subsurface flow constructed wetland treating urban
708 wastewater. Sci. Total Environ. 584-585, 642-650.

709 Pelissari, C., dos Santos, M.O., Rousso, B.Z., Bento, A.P., de Armas, R.D.,
710 Sezerino, P.H., 2016. Organic load and hydraulic regime influence over the

711 bacterial community responsible for the nitrogen cycling in bed media of vertical
712 subsurface flow constructed wetland. Ecol. Eng. 95, 180–188.

713 Saeed, T., Sun, G., 2012. A review on nitrogen and organics removal
714 mechanisms in subsurface flow constructed wetlands: dependency on
715 environmental parameters, operating conditions and supporting media. J.
716 Environ. Manage. 112, 429–448.

717 Saeed, T., Sun, G., 2017. Pollutant Removals Employing Unsaturated and
718 Partially Saturated Vertical Flow Wetlands: A Comparative Study. Chem. Eng. J.
719 325, 332–341.

720 Samad, S., Bakken, L.R., Nadeem, S., Clough, T.J., De, C.A.M., 2016. High-
721 resolution denitrification kinetics in pasture soils link N_2O emissions to pH , and
722 denitrification to C mineralization. PlosOne. 18, 1–11.

723 Sanford, R. A., Wagner D. D., Wu Q., Chee-Sanford J. C., Thomas S. H., Cruz-
724 Garcia C., Rodríguez, G., Massol-Deyá, A., Krishnani, K.K., Ritalaht, M. K.,
725 Nissen, F., KonstantinidiA, K.K., Löffler, F.E., 2012. Unexpected nondenitrifier
726 nitrous oxide reductase gene diversity and abundance in soils. Proc. Natl. Acad.
727 Sci. U.S.A. 109, 19709–19714.

728 Schramm A., Santegoeds C.M., Nielsen H.K., Ploug H., Wagner M., Pribyl M.,
729 Wanner J., Amann R., De Beer D.,1999. On the occurrence of anoxic
730 microniches, denitrification, and sulfate reduction in aerated activated sludge.
731 Appl. Environ. Microb. 65, 4189–4196.

Sezerino, P.H., Bento, A.P., Decezaro, S.T., Carissimi, E., Philippi, L.S., 2012. Constructed wetlands and sand filter applied as onsite post-treatment of anaerobic effluent. Water Pract. Technol. 7, 1–9.

Starkenburg, S.R., Arp, D.J., Bottomley, P.J., 2008. Expression of a putative nitrite reductase and the reversible inhibition of nitrite-dependent respiration by nitric oxide in *Nitrobacter winogradskyi* Nb-255. Environ Microbiol.10, 3036–3042.

Statsoft Inc, 2004. STATISTICA. Data Analysis Software System, Version 7.

Stempfhuber, B., Richter-Heitmann, T., Regan, K.M., Kölbl, A., Wüst, P.K., Marhan, S., Sikorski, J., Overmann, J., Friedrich, M.W., Kandeler, E., Schloter, M., 2015. Spatial Interaction of Archaeal Ammonia-Oxidizers and Nitrite-Oxidizing Bacteria in an Unfertilized Grassland Soil. Front. Microbiol. 6, 1567.

Stieglmeier, M., Mooshammer, M., Kitzler, B., Wanek, W., Zechmeister-Boltenstern, S., Richter, A., & Schleper, C., 2014. Aerobic nitrous oxide production through N-nitrosating hybrid formation in ammonia-oxidizing archaea. The Isme Journal, 8, 1135.

Tietz, A., Hornek, R., Langergraber, G., Kreuzinger, N., Haberl, R., 2007. Diversity of ammonia oxidizing bacteria in a vertical flow constructed wetland. Water Sci. and Technol. 56, 241–247.

Vymazal, J., 2013. The use of hybrid constructed wetlands for wastewater treatment with special attention to nitrogen removal: a review of a recent development. Water Res. 47, 4795–811.

754 Wang, Q., Xie, H., Zhang, J., Liang, S., Ngo, H.H., Guo, W., Liu, C., Zhao, C., Li,
755 H., 2015. Effect of plant harvesting on the performance of constructed wetlands
756 during winter : radial oxygen loss and microbial characteristics. Environ. Sci. and
757 Pollution Res. 22, 7476–7484.

758 Webster, G., Embley, T.M., Prosser, J.I., 2002. Grassland management regimes
759 reduce small-scale het- erogeneity and species diversity of b-proteobacterial
760 ammonia oxidiser populations. Appl. Environ. Microbiol. 68, 20–30.

761 WEF - Water Environment Federation. 2010. Nutrient Removal. Alexandria: Mc
762 Graw Hill. 676 pp.

763 Wu, S., Kuschk, P., Brix, H., Vymazal, J., Dong, R., 2014. Development of
764 constructed wetlands in performance intensifications for wastewater treatment: A
765 nitrogen and organic matter targeted review. Water Res. 57, 40–55.

766 Wunderlin, P., Mohn, J., Joss, A., Emmenegger, L., Siegrist, H. 2012.
767 Mechanisms of N_2O production in biological wastewater treatment under nitrifying
768 and denitrifying conditions. Water Res. 46, 1027–1037.

769 Yoon, S., Nissen, S., Park, D., Sanford, R.A., Loffler, F.E., 2016. Nitrous oxide
770 reduction kinetics distinguish bacteria harboring clade I nosZ from those
771 harboring clade II nosZ. App. Envir. Microbiol. 82, 3793–3800.

FIGURES

a

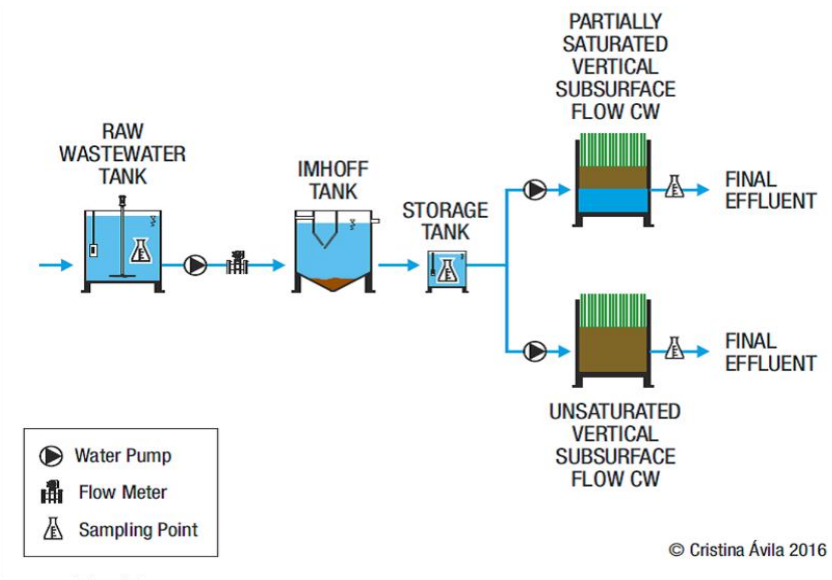

b

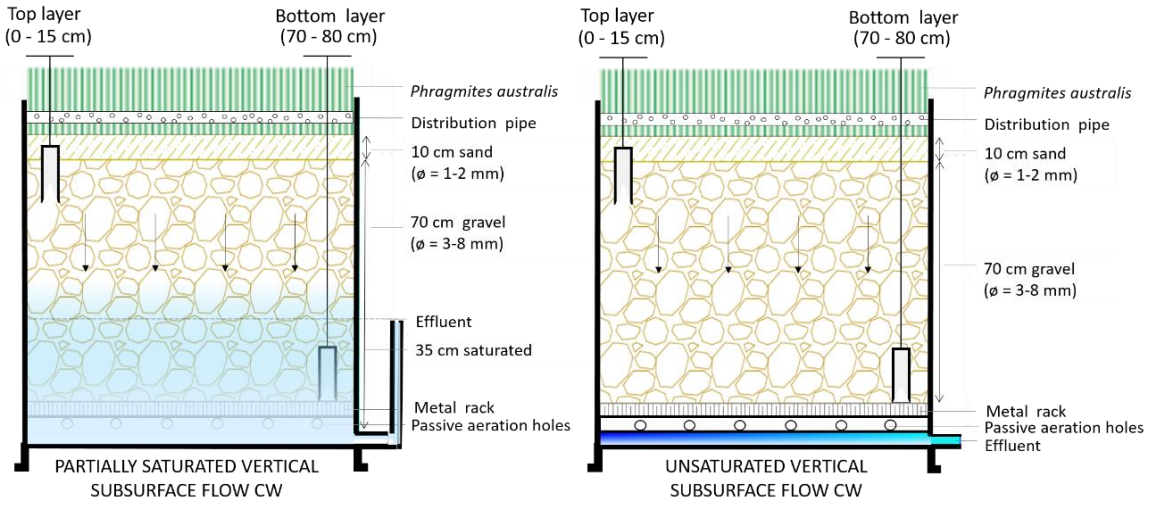

Figure 1. Wastewater treatment plant. (a) Diagram of the experimental treatment plant indicating water influent and effluent sampling points; (b) Cross-section of the two constructed wetlands indicating the gravel (biofilm) sampling depths for microbial analysis.

a

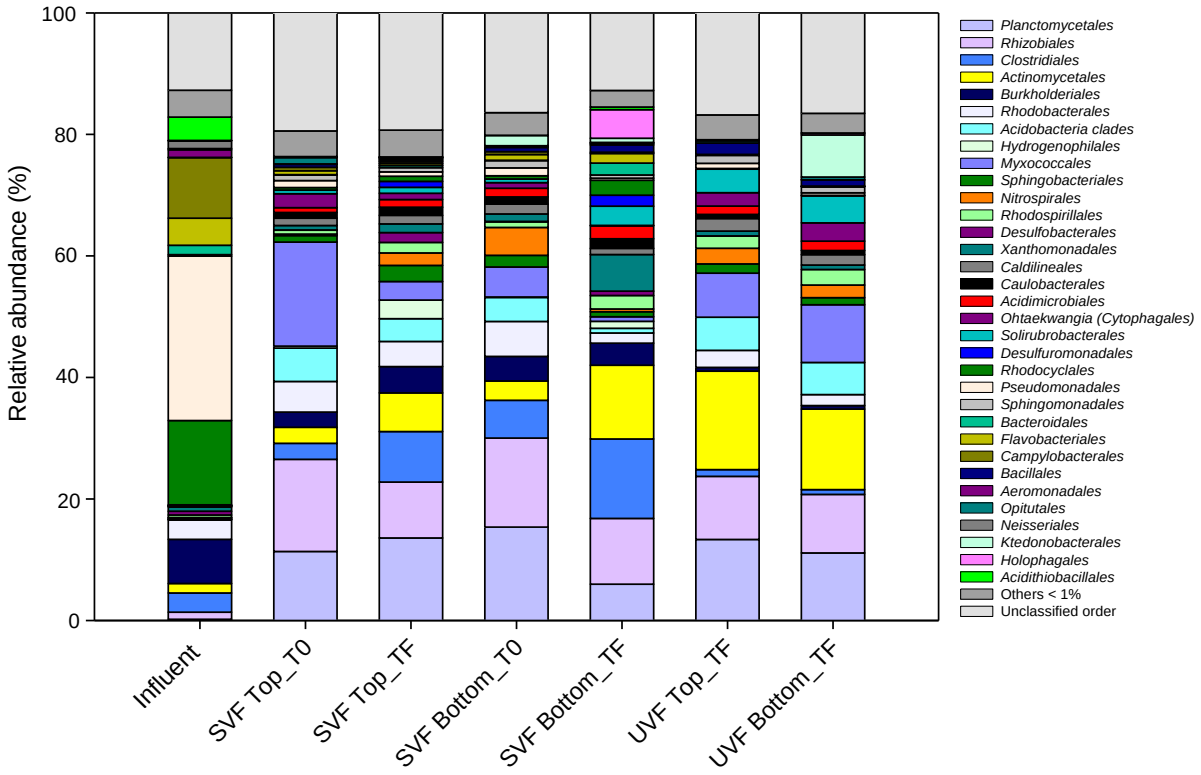

b

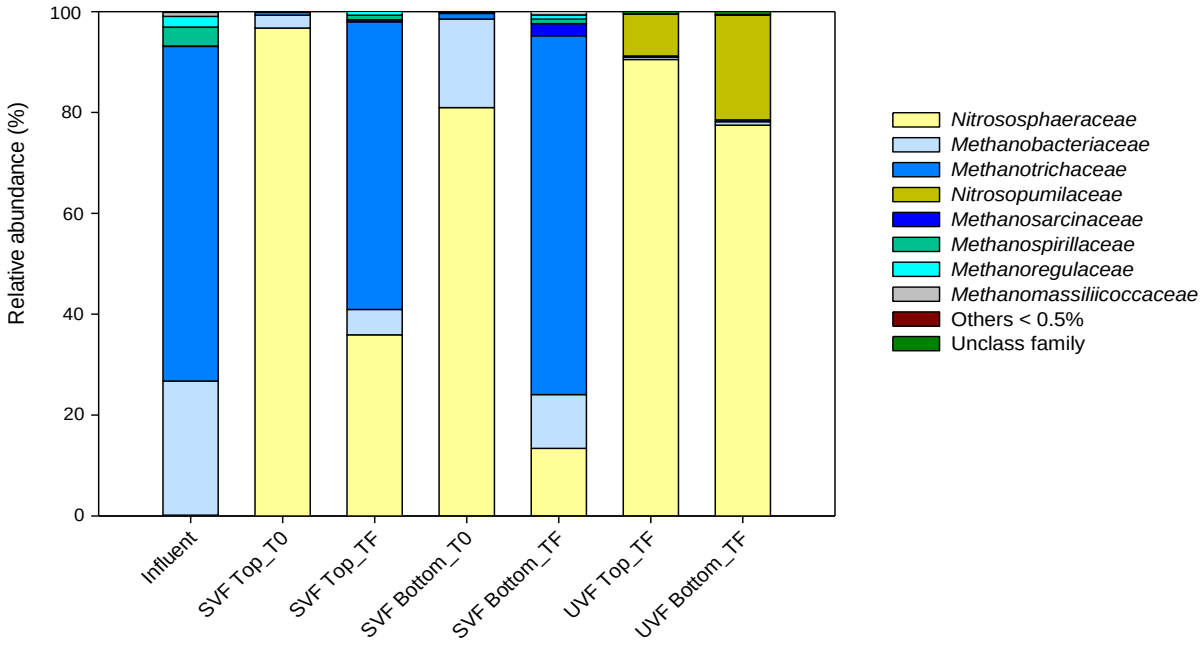

Figure 2. Taxonomic assignment of sequencing reads from the metabolically active bacterial and archaeal communities (cDNA) of influent, and biofilm from top and bottom layers of the unsaturated (UVF) and partially saturated (SVF) vertical flow wetlands. (a) Bacterial community at order level; (b) Archaeal community at family level. Relative abundance was defined by the number of reads (sequences) affiliated with any given taxon, divided by the total number of reads per sample. Phylogenetic groups with relative abundance lower than 1 and 0.5 % were categorized as others.

a

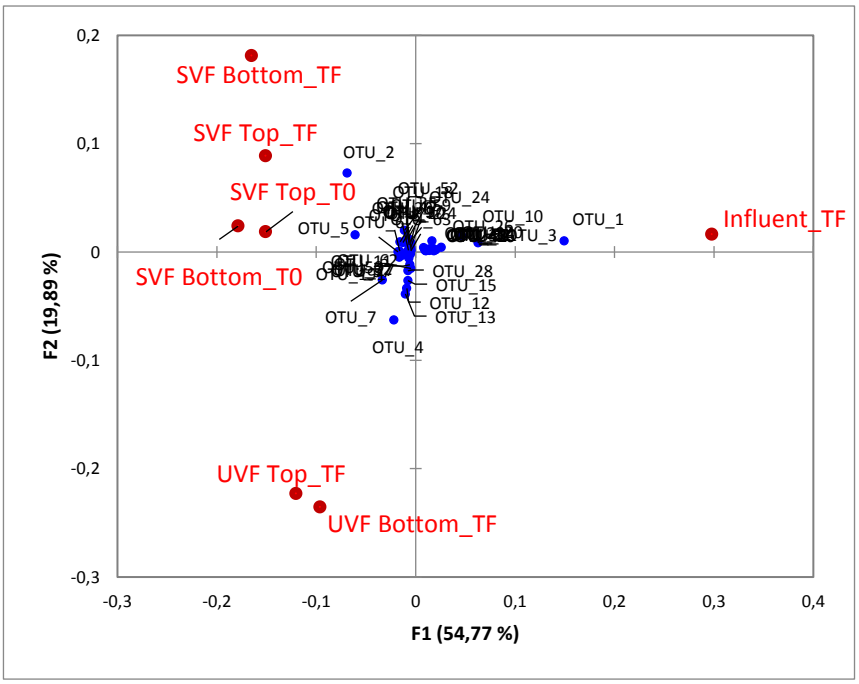

b

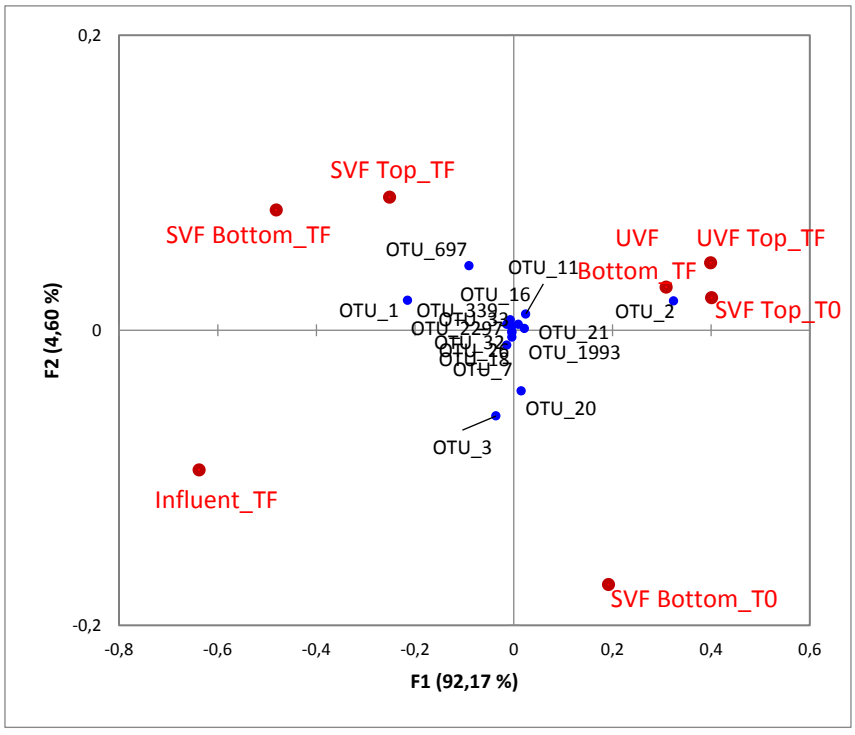

Figure 3. Multivariate Correspondence Analysis (MCA) of the influent wastewater, at initial time (T0) and end time (TF) of the microbial biofilm established on the filter media of the unsaturated (UVF) and partially saturated (SVF) wetlands, in top and bottom layers for cDNA-16S rRNA samples regarding (a) Bacteria; (b) Archaea. (OTUs distribution >1% RA at least in one sample).

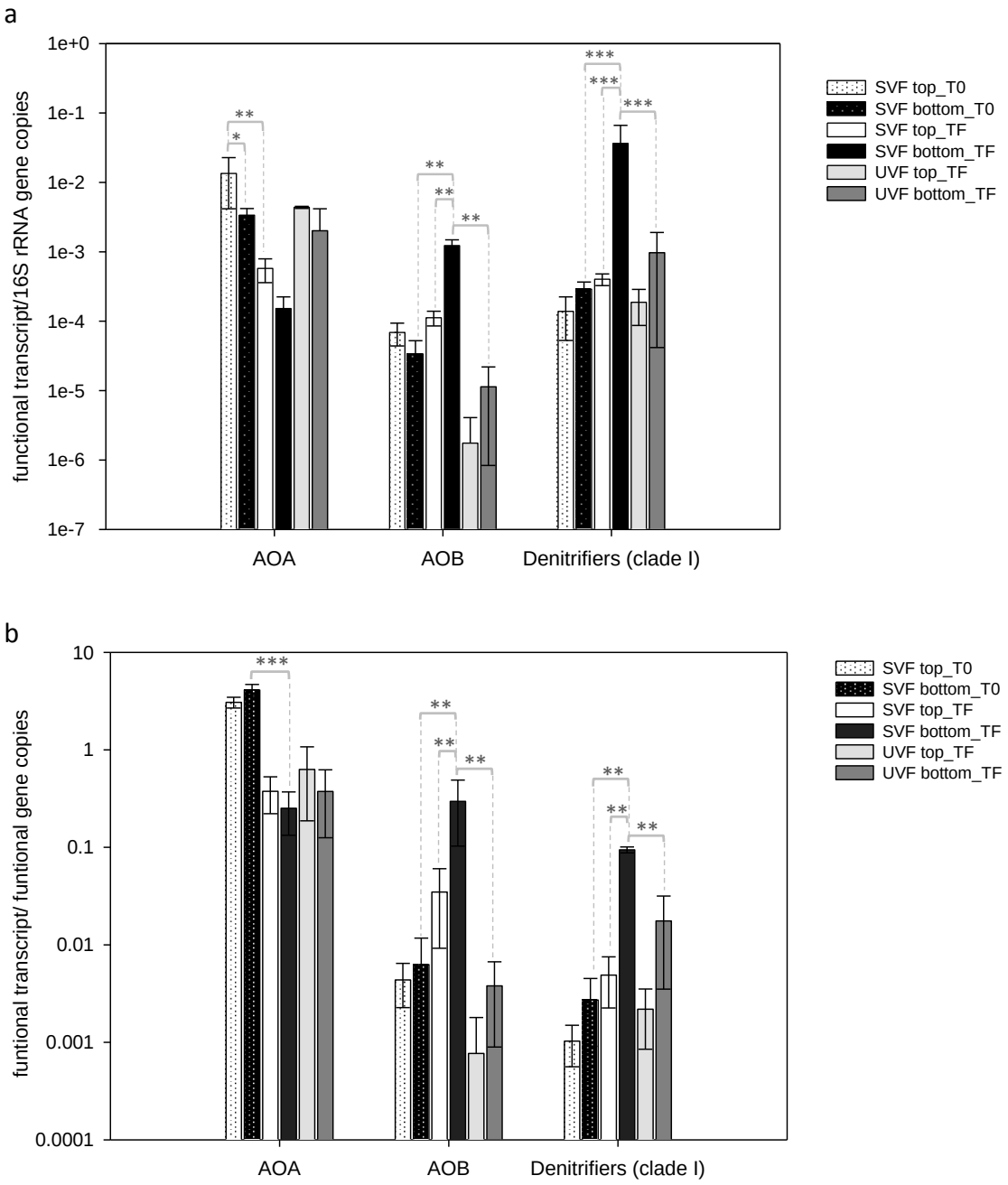

Figure 4**.** Bar charts represent the (RT)-qPCR results of the functional transcripts and genes of *amoA*_AOA (AOA), *amoA*_AOB (AOB) and *nosZ* (denitrifiers-clade I) from bottom and top layers of unsaturated (UVF) and partially saturated vertical (SVF) flow wetlands at different sampling periods, in the case of SVF wetland (initial time (T0) and ending time (TF)) and TF for UVF wetland. (a) Each functional transcript normalized to 16S rRNA gene copies; (b) Each functional transcript versus each functional gene (activity ratio). Presented values are the mean and SD of independent triplicates. * P ≤ 0.05; ** P ≤ 0.01; *** P ≤ 0.001: statistically significant differences of pairwise comparisons (Fisher's least significant difference).

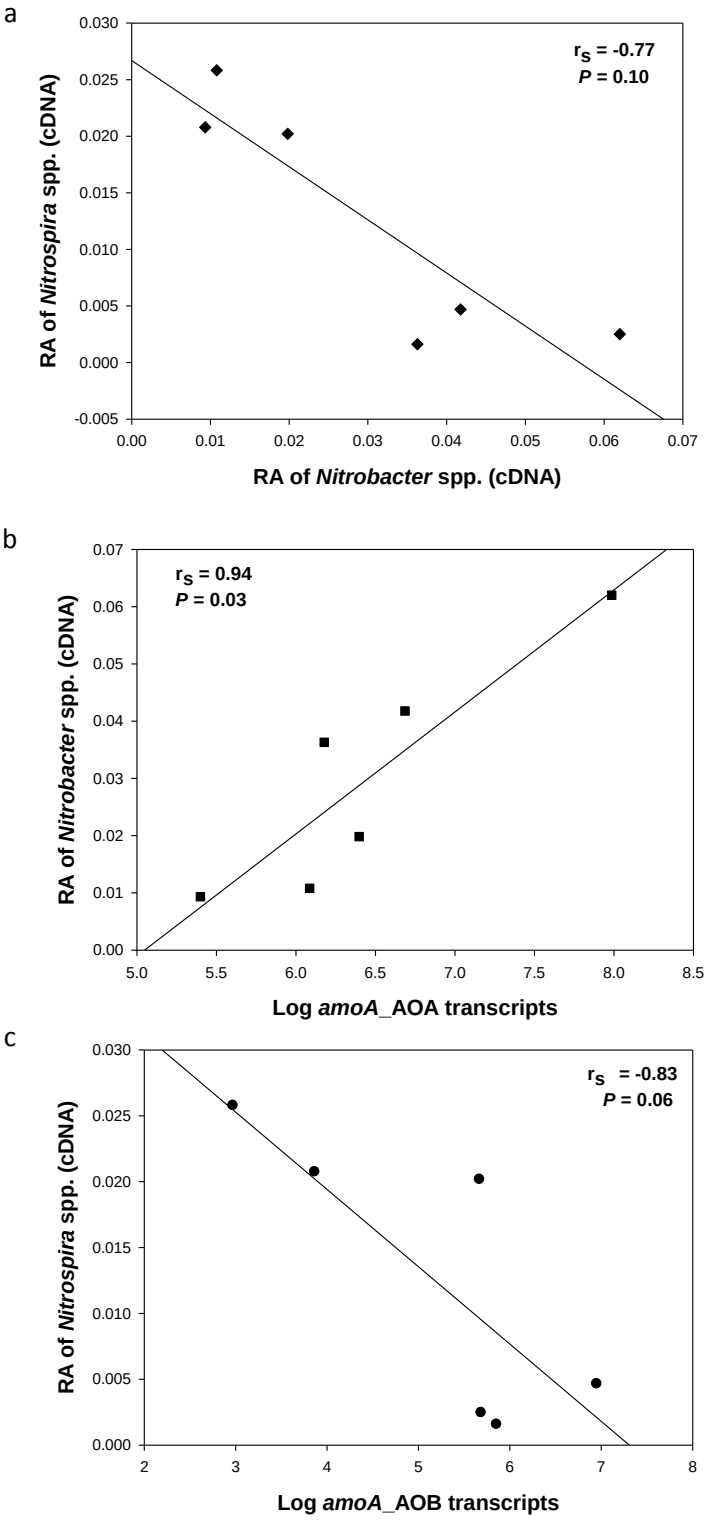

Figure 5. Correlation plots between nitrifying populations. (a) Relative abundances (RA) of active *Nitrobacter* spp. and *Nitrospira* spp.; (b) Active AOA population and RA of active *Nitrobacter* spp.; (c) Active AOB population and RA of active *Nitrospira* spp. Data used in this figure is referred to the starting and ending periods for both wetlands (T0 and TF) and the top and bottom layers of the unsaturated vertical (UVF) and the top layer of the partially saturated vertical (SVF) flow wetlands. The qPCR and NGS data of the previous study (Table S1) conducted in the UVF wetland (Pelissari et al., 2017b) was also included.

TABLES

Table 1. Average (standard deviation) of concentrations, loads of wastewater quality parameters and hydraulic balance at the influent and effluent of the unsaturated (UVF) and partially saturated (SVF) vertical flow wetlands of the six month of operation (January to July 2016).

Parameters (n=33)	**Influent**	**Effluent**		**Significant (*P* < 0.05) pairwise tests**
	wastewater	**UVF wetland**	**SVF wetland**	
T^a (ºC)	16.81 (4.61)	16.15 (4.09)	17.44 (4.84)	ns
DO (mg L^{-1})	0.42 (0.31)	2.20 (0.92)	0.62 (0.45)	A, C
EC (mS cm^{-1})	2.30 (0.78)	2.36 (0.40)	2.65 (0.51)	ns
E_H (mV)	-24.11 (45.99)	90.93 (47.57)	-5.39 (39.45)	A, C
pH	7.33 (0.20)	7.43 (0.21)	6.93 (0.21)	B, C
TSS (mg L^{-1})	102.17 (40.49)	26.23 (18.50)	35.66 (16.64)	A, B
ALR (g m^{-2} d^{-1})	13.41 (5.46)	-	-	-
LRR (g m^{-2} d^{-1})	-	10.05 (5.65)	9.67 (5.46)	ns
LRE (%)	-	71.90 (23.21)	67.82 (18.44)	ns
COD (mg L^{-1})	315.20 (82.11)	105.79 (65.23)	121.59 (45.79)	A, B
ALR (g m^{-2} d^{-1})	41.02 (11.44)	-	-	-
ARR (g m^{-2} d^{-1})	-	26.78 (12.42)	27.55 (11.20)	ns
LRE (%)	-	63.76 (19.84)	66.04 (16.31)	ns
TOC (mg L^{-1})	109.24 (63.80)	33.35 (13.09)	51.18 (18.03)	A, B, C
TN (mg L^{-1})	**60.36 (12.20)**	**41.18 (6.50)**	**33.21 (8.15)**	A, B, C
ALR (g m^{-2} d^{-1})	8.37 (1.37)	-	-	-
LRR (g m^{-2} d^{-1})	-	**2.94 (1.18)**	**4.91 (1.63)**	D
LRE (%) [d]	-	**34.21 (10.79)**	**56.33 (11.32)**	D
NH_4-N (mg L^{-1})	18.68 (4.36)	6.00 (3.02)	6.54 (4.42)	A, B
ALR (g m^{-2} d^{-1})	2.52 (0.60)	-	-	-
LRR (g m^{-2} d^{-1})	-	1.75 (0.54)	1.85 (0.84)	ns
LRE (%)	-	68.21 (17.52)	69.23 (23.48)	ns
NO_x-N (mg L^{-1})	0.13 (0.36)	26.24 (7.85)	0.89 (0.94)	A, C
SO_4^{2-} (mg L^{-1})	105.03 (26.26)	122.39 (21.54)	59.65 (44.46)	B, C
ALR (g m^{-2} d^{-1})	13.72 (3.45)	-	-	-
LRR (g m^{-2} d^{-1})	-	-2.41 (3.64)	7.90 (6.20)	D
LRE (%)	-	-16.98 (32.77)	61.76 (25.54)	D
Hydraulic balance (n=100)				
Flow (L d^{-1})	200.22 (1.02)	198.39 (2.43)	173.90 (5.84)	A, B, C
Evapotranspiration (mm d^{-1})	-	1.22 (1.75)	17.55 (3.90)	D
Evapotranspiration (%)	-	0.91 (1.31)	13.71 (2.68)	D

Note: Applied Load Rate (ALR); Load Rate Removal (LRR); Load Removal Efficiency (LRE). Letters represent significant differences (Friedman test) between influent and UVF effluent (A), influent and SVF effluent (B) and UVF and SVF effluents (C), respectively. Letter D represent significant differences (Wilcoxon signed rank test) between UVF and SVF effluents. ns: $P > 0.05$.

Table 2. Average (standard deviation) of alpha diversity indexes for metabolically active bacteria and archaea populations in the influent wastewater and in the microbial biofilm established on the filter media of the unsaturated (UVF) and partially saturated (SVF) vertical flow wetlands at initial time (T0) and end time (TF) in the top and bottom layers (mean ± SD). Data normalized by using contigs close to the sample with the lowest number of contigs (50,000 and 25,000 reads (contigs) for eubacteria and archaea, respectively).

	Reads (contigs)	Coverage[1]	OTUs[1]	Chao1[1]	Shannon[1]	Inv.Simpson[1]
Bacteria						
Influent_TF	72023	0.9881 (0.0003)	1587 (13)	2333 (67)	4.250 (0.006)	14.92 (0.09)
SVF Top_T0	60912	0.9800 (0.0004)	3484 (12)	4319 (53)	6.459 (0.004)	138.43 (0.98)
SVF Top_TF	56415	0.9777 (0.0003)	3613 (11)	4685 (52)	6.452 (0.003)	149.58 (0.75)
UVF Top_TF	58783	0.9805 (0.0003)	3720 (12)	4538 (46)	6.770 (0.003)	210.74 (1.47)
SVF Bottom_T0	59290	0.9777 (0.0003)	3913 (13)	4831 (49)	6.645 (0.004)	163.98 (0.98)
SVF Bottom_TF	63940	0.9805 (0.0004)	3275 (14)	4165 (58)	6.268 (0.004)	95.25 (0.76)
UVF Bottom_TF	64375	0.9802 (0.0004)	3702 (14)	4509 (53)	6.632 (0.004)	180.78 (1.27)
Archaea						
Influent_TF	122818	0.9988 (0.0002)	105 (4)	138 (18)	1.50 (0.010)	2.43 (0.02)
SVF Top_T0	55263	0.9989 (0.0002)	72 (3)	100 (14)	0.63 (0.006)	1.34 (0.00)
SVF Top_TF	97873	0.9986 (0.0002)	116 (5)	158 (20)	1.74 (0.008)	3.73 (0.02)
UVF Top_TF	25978	0.9990 (5E-05)	82 (1)	108 (6)	0.76 (0.002)	1.41 (0.00)
SVF Bottom_T0	42921	0.9987 (0.0002)	95 (3)	129 (16)	1.33 (0.006)	2.40 (0.01)
SVF Bottom_TF	70800	0.9986 (0.0002)	124 (4)	161 (17)	2.02 (0.008)	4.24 (0.03)
UVF Bottom_TF	29241	0.9990 (0.0001)	84 (2)	110 (10)	1.08 (0.004)	1.84 (0.00)